

Use of CAV in Determining Effects of Small Magnitude Earthquakes on Seismic Hazard Analyses

[Product ID #]

DRAFT Final Report, June 2006

Cosponsor
U.S. Department of Energy
Office of Nuclear Energy Sciences & Technology
19901 Germantown Road, NE-20
Germantown, MD, 20874-1290

EPRI Project Managers
R. Kassawara and L. Sandell

DISCLAIMER OF WARRANTIES AND LIMITATION OF LIABILITIES

THIS DOCUMENT WAS PREPARED BY THE ORGANIZATION(S) NAMED BELOW AS AN ACCOUNT OF WORK SPONSORED OR COSPONSORED BY THE ELECTRIC POWER RESEARCH INSTITUTE, INC. (EPRI). NEITHER EPRI, ANY MEMBER OF EPRI, ANY COSPONSOR, THE ORGANIZATION(S) BELOW, NOR ANY PERSON ACTING ON BEHALF OF ANY OF THEM:

(A) MAKES ANY WARRANTY OR REPRESENTATION WHATSOEVER, EXPRESS OR IMPLIED, (I) WITH RESPECT TO THE USE OF ANY INFORMATION, APPARATUS, METHOD, PROCESS, OR SIMILAR ITEM DISCLOSED IN THIS DOCUMENT, INCLUDING MERCHANTABILITY AND FITNESS FOR A PARTICULAR PURPOSE, OR (II) THAT SUCH USE DOES NOT INFRINGE ON OR INTERFERE WITH PRIVATELY OWNED RIGHTS, INCLUDING ANY PARTY'S INTELLECTUAL PROPERTY, OR (III) THAT THIS DOCUMENT IS SUITABLE TO ANY PARTICULAR USER'S CIRCUMSTANCE; OR

(B) ASSUMES RESPONSIBILITY FOR ANY DAMAGES OR OTHER LIABILITY WHATSOEVER (INCLUDING ANY CONSEQUENTIAL DAMAGES, EVEN IF EPRI OR ANY EPRI REPRESENTATIVE HAS BEEN ADVISED OF THE POSSIBILITY OF SUCH DAMAGES) RESULTING FROM YOUR SELECTION OR USE OF THIS DOCUMENT OR ANY INFORMATION, APPARATUS, METHOD, PROCESS, OR SIMILAR ITEM DISCLOSED IN THIS DOCUMENT.

ORGANIZATION(S) THAT PREPARED THIS DOCUMENT

ARES Corporation, Inc.
Norm A. Abrahamson, Inc.

NOTE

For further information about EPRI, call the EPRI Customer Assistance Center at 800.313.3774 or e-mail askepri@epri.com.

Electric Power Research Institute and EPRI are registered service marks of the Electric Power Research Institute, Inc.

Copyright © 2006 Electric Power Research Institute, Inc. All rights reserved.

CITATIONS

This report was prepared by

Norm A. Abrahamson, Inc.
152 Dracena Avenue
Piedmont, CA 92707

Principal Investigators
N. Abrahamson
J. Watson-Lamprey

ARES Corporation, Inc.
5 Hutton Centre Drive
Suite 610
Santa Ana, CA 92707

Principal Investigators
G. Hardy
K. Merz

This report describes research sponsored by the Electric Power Research Institute (EPRI) and the U.S. Department of Energy under Award No. (DE-FC07-04ID14533).

This publication is a corporate document that should be cited in the literature in the following manner:

Use of CAV in Determining Effects of Small Magnitude Earthquakes on Seismic Hazard Analysis. EPRI, Palo Alto, CA and the U.S. Department of Energy: 2006 <Product ID Number>.

PRODUCT DESCRIPTION

This study provides the technical basis for establishing the appropriate distribution of low magnitude earthquakes for use in probabilistic seismic hazard computations for nuclear power plant applications.

Approach

Current seismic hazard methods generally utilize a lower bound magnitude cut-off level which was a conservatively defined value based on several past research studies whose objective was to estimate the damage potential of small earthquakes. A much more complete and technically defensible characterization of the damage potential for small earthquakes was determined to be the cumulative absolute velocity (CAV). A CAV value of 0.16 g-sec was defined in past studies to characterize a conservative estimate of the threshold between damaging earthquake motions and non-damaging earthquake motions for well-engineered structures. Based on the review of available CEUS and WUS data, this study develops a CAV model as a function of the uniform duration, magnitude, peak ground acceleration, and site shear wave velocity.

Results and Findings

The application of a minimum CAV value significantly reduces the contribution of small magnitude earthquakes to the total hazard. An example application was performed within this study. The magnitude of the dominant earthquake is shown to increase from 5.25 to 5.8 by applying the minimum CAV as a filter. This example shows that the past PSHA studies that used a minimum moment magnitude of 4.6 can overestimate the hazard by including earthquakes that are not damaging but which contribute significantly to the hazard when they are located at short distances from the site.

EPRI Perspective

Modern seismic hazard studies within the CEUS have typically exhibited increasing levels of ground motion (for a given return period), particularly in the high frequency part of the spectrum. A significant part of this increase can be traced to smaller magnitude earthquakes which previous EPRI studies have shown not to be damaging to nuclear plant structures and equipment. The application of a minimum CAV value significantly reduces the contribution of small magnitude earthquakes to the total hazard and results in a much more realistic seismic hazard characterization for use in defining design earthquake levels for new nuclear power plants or for assessing the seismic adequacy of existing plants.

Keywords

Cumulative Absolute Velocity (CAV)

Lower Bound Magnitude Earthquakes

Probabilistic Seismic Hazard Analysis (PSHA)

Seismic Hazard

Seismic Probabilistic Risk Assessment

ABSTRACT

This study provides the technical basis for establishing the appropriate distribution of low magnitude earthquakes for use in probabilistic seismic hazard computations for nuclear power plant applications. Current seismic hazard methods generally utilize a lower bound body wave magnitude cut-off value of 5.0 (approximate moment magnitude of 4.6) to integrate the probabilistic seismic hazard. This lower bound magnitude cut-off level is a conservatively defined value, based on several past EPRI studies, which is used to remove small earthquakes with low damage potential from the probabilistic seismic hazard analysis. Other research has been conducted by EPRI to determine the single ground motion measure that is best correlated with threshold of potential damage to engineered structures. Several ground motion measures such as peak ground acceleration, Arias intensity, root mean square acceleration, and cumulative absolute velocity (CAV) were evaluated in the process of selecting the best parameter for use in predicting the threshold of potential damage. The CAV was determined to be the best parameter and a CAV value of 0.16 g-sec was found to be a conservative characterization of the threshold between damaging earthquake motions and non-damaging earthquake motions for buildings of good design and construction as defined by the Modified Mercalli Scale.

In this study, a model for CAV is proposed based on both the ground motion parameter and the earthquake parameters. The CAV model is developed based on the extensive strong motion data set from the western United States (WUS) in two steps. In the first step, CAV is modeled as a function of the uniform duration, magnitude, peak ground acceleration, and site shear wave velocity. In the second step, the uniform duration is modeled as a function of the peak ground acceleration, magnitude, and site shear wave velocity. Taken together, these two steps lead to a model of CAV that depends on parameters that are available in a standard PSHA. Comparisons with a small set of ground motions from earthquakes in the central and eastern United States (CEUS) and Canada show that the CAV model and the duration model developed from the WUS data sets are also applicable to the CEUS earthquakes. An example application of the CAV filtering to seismic hazard in the CEUS is shown. The application of a minimum CAV value significantly reduces the contribution of small magnitude earthquakes to the total hazard. The magnitude of the dominant earthquake is shown to increase from 5.25 to 5.8 by applying the minimum CAV as a filter. This example shows that the past PSHA studies that used a minimum moment magnitude of 4.6 can overestimate the hazard by including earthquakes that are not damaging but which contribute significantly to the hazard when they are located at short distances from the site.

CONTENTS

1 INTRODUCTION	1-1
Use of Lower Bound CAV in PSHA.....	1-3
2 EMPIRICAL MODEL OF CAV.....	2-1
Empirical Data Set for WUS	2-1
Empirical Data Set for EUS.....	2-3
Model for CAV Based on WUS Data – 2-Step Approach.....	2-6
Step 1 – Model for CAV Including Duration Dependence	2-8
Step 2 – Model for Uniform Duration	2-14
Combined Model for CAV.....	2-23
Probability of Exceeding Specified CAV Value.....	2-26
Model for CAV Based on Combined WUS/CEUS/Canadian Data – 1-Step Approach	2-27
3 APPLICATION OF THE CAV MODEL FOR RESPONSE SPECTRAL VALUES	3-1
Independent CAV Models for Spectral Acceleration	3-1
CAV Models for Spectral Acceleration Correlated to PGA.....	3-1
4 METHODOLOGY FOR APPLICATION OF MINIMUM CAV IN SEISMIC HAZARD ANALYSES	4-1
Application of CAV Filtering During the Hazard Calculation.....	4-1
Application of CAV Filtering in the Post Processing of the Hazard Calculation	4-1
5 EXAMPLE APPLICATION	5-1
6 CONCLUSIONS	6-1
7 REFERENCES	7-1
APPENDIX A COMMENTS AND RESPONSES TO NRC REQUESTS FOR ADDITIONAL INFORMATION (RAIs).....	A-1

APPENDIX B EMPIRICAL EARTHQUAKE DATA SETS USED FOR CAV MODELS..... B-1

LIST OF FIGURES

Figure 1-1 Example of Deaggregation for EUS Source Zones for 20 Hz Spectral Acceleration.	1-2
Figure 1-2 Example Showing the Correlation of the PGA and CAV for a Narrow Range of Magnitudes (6.5-7.0), Distances (15-30 km), and Site Conditions (360-VS30<760 m/s)	1-4
Figure 1-3 Comparison of the PDF for PGA (Blue Curve) and the PGA PDF Scaled by the Probability of CAV>0.16g-s (Red Curve) Assuming Independence of the PGA and CAV	1-5
Figure 1-4 Comparison of the PDF for PGA (Blue Curve) and the PGA PDF Scaled by the Probability of CAV>0.16g-s (Red Curve)	1-5
Figure 2-1 Distribution of Earthquake Magnitudes and Distances for the WUS Data Set	2-2
Figure 2-2 Distribution of V_{S30} Values for the WUS Data Set	2-2
Figure 2-3 Dependence of the CAV on the PGA and Magnitude	2-7
Figure 2-4 Duration Dependence of the CAV	2-7
Figure 2-5 Residuals of Initial CAV Model (Equation 2-1) as a Function of Magnitude	2-8
Figure 2-6 Residuals of Initial CAV Model (Equation 2-1) as a Function of PGA	2-9
Figure 2-7 Residuals of Initial CAV Model (Equation 2-1) as a Function of V_{S30}	2-9
Figure 2-8 Median CAV Model for $V_S=600$ m/s for Different PGA Values	2-11
Figure 2-9 Median CAV Model for $V_S=600$ m/s for Different Magnitudes	2-11
Figure 2-10 Duration Dependence of the CAV Residuals	2-12
Figure 2-11 Magnitude Dependence of the CAV Residuals	2-12
Figure 2-12 PGA Dependence of the CAV Residual	2-13
Figure 2-13 V_{S30} Dependence of the CAV Residual	2-13
Figure 2-14 CAV Residuals for CEUS/Canadian Data Using the Observed Uniform Durations	2-14
Figure 2-15 Dependence of the Uniform Duration with PGA	2-15
Figure 2-16 Dependence of the Uniform Duration with Magnitude	2-15
Figure 2-17 Magnitude Dependence of the Residuals of the Uniform Duration from the Initial Model for WUS Data	2-16
Figure 2-18 V_{S30} Dependence of the Residuals of the Uniform Duration from the Initial Model for WUS Data	2-16
Figure 2-19 Distance Dependence of the Residuals of the Uniform Duration from the Initial Model for WUS Data	2-17
Figure 2-20 Median Uniform Duration for $V_{S30}=600$	2-18

Figure 2-21 PGA Dependence of the Uniform Duration Residuals	2-19
Figure 2-22 Magnitude Dependence of the Uniform Duration Residuals	2-20
Figure 2-23 Distance Dependence of the Uniform Duration Residuals	2-20
Figure 2-24 Shear-Wave Velocity Dependence of the Uniform Duration Residuals.....	2-21
Figure 2-25 PGA Dependence of the Uniform Duration Residuals from the ENA Ground Motions Listed in Table 2-2	2-21
Figure 2-26 V_{S30} Dependence of the Uniform Duration Residuals from the ENA Ground Motions Listed in Table 2-2	2-22
Figure 2-27 Magnitude Dependence of the Uniform Duration Residuals from the ENA Ground Motions Listed in Table 2-2	2-22
Figure 2-28 Distance Dependence of the Uniform Duration Residuals from the ENA Ground Motions Listed in Table 2-2	2-23
Figure 2-29 Standard Deviation of the $\ln(\text{CAV})$ if the Median Duration Model is Used	2-24
Figure 2-30 PGA Dependence of the ENA CAV Residuals Using the Median Duration.....	2-24
Figure 2-31 Magnitude Dependence of the ENA CAV Residuals Using the Median Duration.....	2-25
Figure 2-32 V_{S30} Dependence of the ENA CAV Residuals Using the Median Duration	2-25
Figure 2-33 Distance Dependence of the ENA CAV Residuals Using the Median Duration.....	2-25
Figure 2-34 Probability of $\text{CAV} > 0.16g\text{-sec}$ for $V_S = 1000\text{m/s}$ Using the Two-Step Approach.....	2-26
Figure 2-35 PGA Dependence of the Residuals of CAV from the Single Step Model	2-28
Figure 2-36 V_{S30} Dependence of the Residuals of CAV from the Single Step Model.....	2-28
Figure 2-37 Magnitude Dependence of the Residuals of CAV from the Single Step Model....	2-28
Figure 2-38 Distance Dependence of the Residuals of CAV from the Single Step Model.....	2-29
Figure 2-39 Comparison of the Probability of $\text{CAV} > 0.16g\text{-s}$ from the Two-Step and One- Step Approaches for $V_{S30} = 1000\text{m/s}$	2-29
Figure 5-1 20 Hz Hazard Computed With and Without CAV Filtering	5-2
Figure 5-2 UHS for $1E-4$ With and Without CAV Filtering.....	5-2
Figure 5-3 Deaggregation of 20 Hz Spectral Acceleration Hazard for $1E-4$	5-3

LIST OF TABLES

Table 2-1 CEUS and Canadian Earthquakes with $M \geq 4$ from the EPRI (1993) Strong Motion Data Set with at Least One Horizontal Component with $PGA > 0.025g$	2-4
Table 2-2 CEUS/CANADIAN Ground Motions with at Least One Horizontal Component with $PGA > 0.025g$	2-5
Table 2-3 Coefficients for CAV Model.....	2-10
Table 2-4 Coefficients for Uniform Duration Model.....	2-18
Table 2-5 Coefficients for Single Step CAV Model	2-27
Table 3-1 Coefficients for the Correlation of the Variability of $\ln(PGA)$ and $\ln(S_a)$	3-2

1 INTRODUCTION

Probabilistic seismic hazard analysis (PSHA) for a site integrates the hazard from all possible earthquakes in the site region that are potentially damaging. In current practice, non-damaging earthquakes are those with magnitudes below a conservatively determined lower bound earthquake magnitude. For these applications, earthquakes above the minimum magnitude are considered to be potentially damaging, and earthquakes below the minimum magnitude are not potentially damaging. This lower bound is included in the PSHA by setting the minimum magnitude in the hazard integral as shown in Equation 1-1.

$$v(Sa > z) = \sum_{i=1}^{N_{source}} N_i(M > M_{min}) \int_{M_{min}}^{M_{max_i}} \int_{r=0}^{\infty} f_{mi}(M) f_{ri}(r, M) P(Sa > z | M, r) dr dM \quad \text{Equation 1-1}$$

where $v(Sa > z)$ is the hazard rate, f_m and f_r are probability density functions describing the distributions of earthquake magnitudes and distances, respectively, and $N_i(M > M_{min})$ is the rate of earthquakes for the i^{th} source. (Note: In Equation 1-1, the ground motion is shown to only depend on M and R for simplicity. Dependencies on the site condition, hypocentral depth, or other parameters can be included as needed and does not impact the general approach.)

A summary of approaches to determining appropriate minimum magnitude to use for buildings of good design and construction as defined by the Modified Mercalli Scale is given in McCann and Reed (1989). Based on that early work, a conservative assumption is that for buildings of good design and construction, a minimum body wave magnitude (m_{bLg}) of 5.0 should be used for PSHA. In the recent EPRI sponsored PSHA for nuclear power plants in the CEUS, a minimum m_{bLg} of 5.0 was used. This minimum m_{bLg} was converted to a minimum moment magnitude of $M = 4.6$. (Note: In this report, M denotes moment magnitude.)

The use of a conservative lower bound magnitude approach has an important negative impact on hazard estimation, causing a bias to high hazard particularly for higher response spectra frequencies. The bias is a consequence of incorporating non-damaging earthquakes into the hazard. These are primarily small magnitude events near the site of interest, which occur with much greater rate than larger magnitude earthquakes because of the exponential increase in the number of earthquakes with decreasing magnitude. As an example, the deaggregation of the 20 Hz spectral hazard for a CEUS rock site, located away from the Charleston and New Madrid source zones, is shown in Figure 1-1. This example hazard determination used a minimum moment magnitude of 4.6.

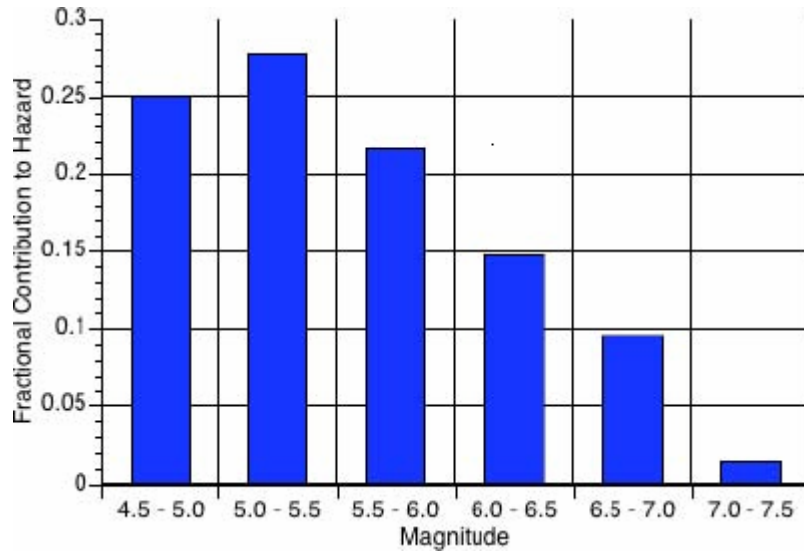


Figure 1-1
Example of Deaggregation for EUS Source Zones for 20 Hz Spectral Acceleration.
There is a large contribution to the hazard from earthquakes near the M=4.6 lower bound magnitude.

Figure 1-1 shows that there is a large contribution from events with magnitudes just above the minimum magnitude. If these small magnitude earthquakes are not potentially damaging, then the computed hazard will be biased to high ground motion values and the determination of the controlling earthquake will be biased to smaller magnitudes and closer distances.

The lower bound magnitude approach used in past seismic hazard modeling is equivalent to assuming that the probability of an earthquake being potentially damaging is a step function. For example, if the minimum moment magnitude is 4.6, then a moment magnitude earthquake of 4.61 has a probability of 1.0 of being potentially damaging, whereas a moment magnitude earthquake of 4.59 has a probability of 0.0 of being potentially damaging. Clearly, the step function is not realistic and does not properly represent the potential for damage as a function of earthquake magnitude. The transition from not potentially damaging to potentially damaging should be a smoother distribution on magnitude.

As an alternative to using earthquake magnitude to determine non-damaging earthquakes, Reed and Kennedy (1988) proposed using the ground motion measure, denoted as CAV, given by the integral of the absolute value of a ground motion acceleration recording. To make the CAV value representative of strong ground shaking rather than coda waves (small amplitudes that can continue on for a long time after the strong shaking), O’Hara and Jacobson (1991) restricted the integration for computing CAV to 1-second time windows that have amplitudes of at least 0.025g. This definition of CAV is given by:

$$CAV = \sum_{i=1}^N H(pga_i - 0.025) \int_{t=t_i}^{t=t_{i+1}} |a(t)| dt$$

Equation 1-2

where N is the number of 1-second time windows in the time series, pga_i is the peak ground acceleration (in g) during time window i , t_i is the start time of time window i , and $H(x)$ is the Heaviside function (unity for $x > 0$ and 0 otherwise).

As shown by O'Hara and Jacobson (1991), a CAV value of 0.16g-sec is associated with a negligible level of observed damage to buildings of good design and construction. Based on the definition in Equation 1-2, the CAV parameter is a measure of the mean deviation of the strong motion portion of the acceleration record times the duration. Although named the "Cumulative Absolute Velocity", the CAV is not directly related to the ground motion velocity (derivative of acceleration), but it does have units of velocity (g -s). The parameter is denoted by the name Cumulative Absolute Velocity since, if it is noted that $a = dv/dt$, the integral in Equation 1-2 may be written as $\sum_j |\Delta v_j|$ or the accumulative changes in velocity minima/maxima within each one second time interval.

Use of Lower Bound CAV in PSHA

If a lower bound value of CAV is used to define potentially damaging earthquakes, then the hazard integral in Equation 1.1 becomes:

$$v(Sa > z, CAV > CAV_{\min}) = \sum_{i=1}^{N_{\text{source}}} N_i (M > M_{\min}) \int_{M_{\min}}^{M_{\max i}} \int_{r=0}^{\infty} f_{mi}(M) f_{ri}(r, M) P(Sa > z, CAV > CAV_{\min} | M, r) dr dM$$

Equation 1-3

The difference in the hazard integral is that instead of the probability of $Sa > z$ for a given M and R , we have the joint probability of $Sa > z$ and $CAV > CAV_{\min}$ for a given M and R . From basic probability theory, the joint probability of x and y is given by:

$$P(x, y) = P(y)P(x | y) = P(x)P(y | x) \quad \text{Equation 1-4}$$

where $P(x|y)$ is the conditional probability of x given y . If x and y are independent, then the joint probability simplifies to $P(x, y) = P(x)P(y)$, but this simplification does not apply if they are not independent.

In Equation 1-3, we have the joint probability of $Sa > z$ and $CAV > CAV_{\min}$. If the spectral acceleration is determined by the M and R through the ground motion attenuation relation and the CAV is determined by M and R , then it is not apparent why we are concerned with the dependence of CAV on Sa . It would appear that the dependence is already accommodated through the M and R variables. The reason we need to consider the dependence is that there is aleatory variability of the ground motion and CAV for a given M and R . The ground motion attenuation relation gives the median and standard deviation of $\ln(Sa)$ for a given M and R . So even if the M and R are known values, there is a large range of ground motions and CAV values

that could occur. Intuitively, if we have a higher than average ground motion, then we expect to also have a higher than average CAV; conversely, if we have a lower than average ground motion, then we expect a lower than average CAV. Therefore, we expect the CAV variability to be correlated with the Sa variability.

As an example, the PGA and CAV from a narrow magnitude and distance range for soft-rock sites are plotted in Figure 1-2. This figure shows that the variability of PGA and CAV values that have been observed for this magnitude, distance and site condition are strongly correlated. For larger PGA values, the CAV values tend to be larger; and for smaller PGA values, the CAV values tend to be smaller. Therefore, the two parameters are not independent.

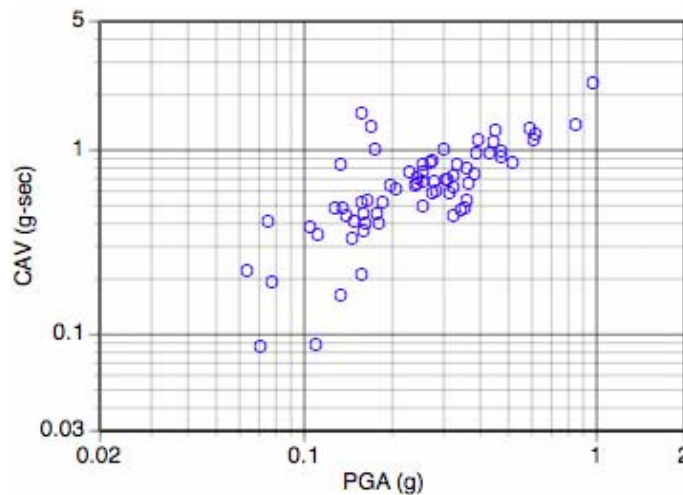


Figure 1-2
Example Showing the Correlation of the PGA and CAV for a Narrow Range of Magnitudes (6.5-7.0), Distances (15-30 km), and Site Conditions (360-VS30<760 m/s)

If this correlation is ignored and the PGA and CAV variability is assumed to be independent, then the hazard will be underestimated. To demonstrate this, consider the ground motion from a single magnitude and distance. For this magnitude and distance, assume that the median PGA is 0.4g and that the probability of $CAV > 0.16g\text{-sec}$ is 0.5. Figure 1-3 shows an example distribution of the PGA. The probability of exceeding a PGA of 0.5g without considering CAV is given by the area under the blue curve to the right of 0.5g. In this case, the probability is 0.38. If the PGA is independent of the CAV, then the distribution of PGA values for $CAV > 0.16g\text{-s}$ is shown by the red curve. With this red curve, the joint probability of the PGA exceeding 0.5g and $CAV > 0.16g\text{-s}$ is 0.19. If we include the correlation of the PGA and CAV, then the distribution of the PGA for $CAV > 0.16g\text{-s}$ is shown by the red curve in Figure 1-4. The total area under the red curve is 0.5 in both Figure 1-3 and 1-4, but including the correlation leads to a larger area above 0.5g. In this case, the joint probability of the PGA exceeding 0.5g and $CAV > 0.16g\text{-s}$ is 0.31, which is larger than the value of 0.19 computed with the assumption that the PGA and CAV are independent.

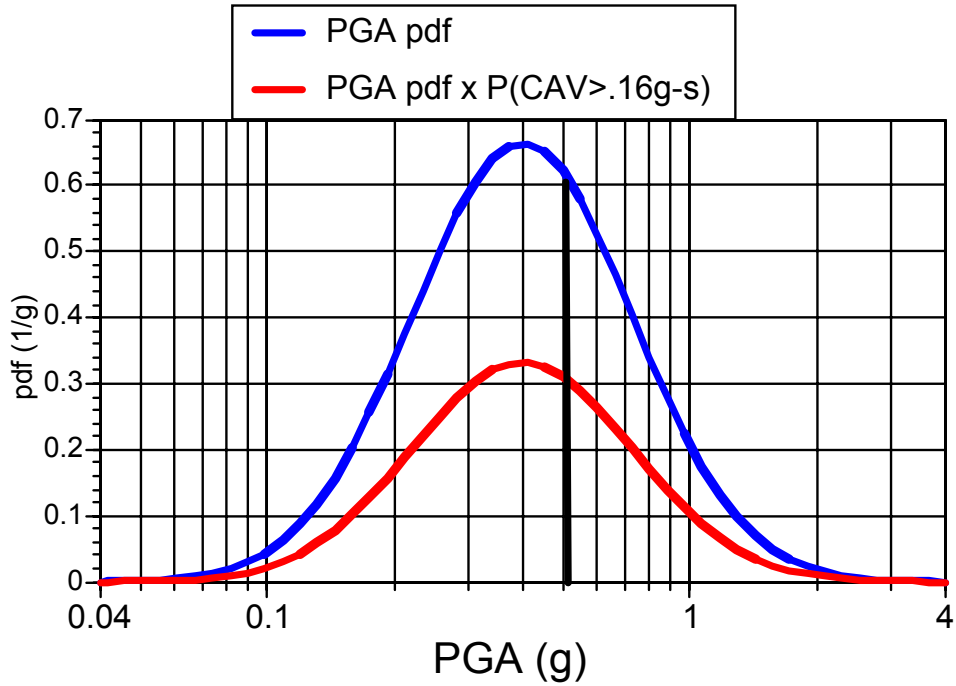


Figure 1-3
 Comparison of the PDF for PGA (Blue Curve) and the PGA PDF Scaled by the Probability of CAV>0.16g-s (Red Curve) Assuming Independence of the PGA and CAV

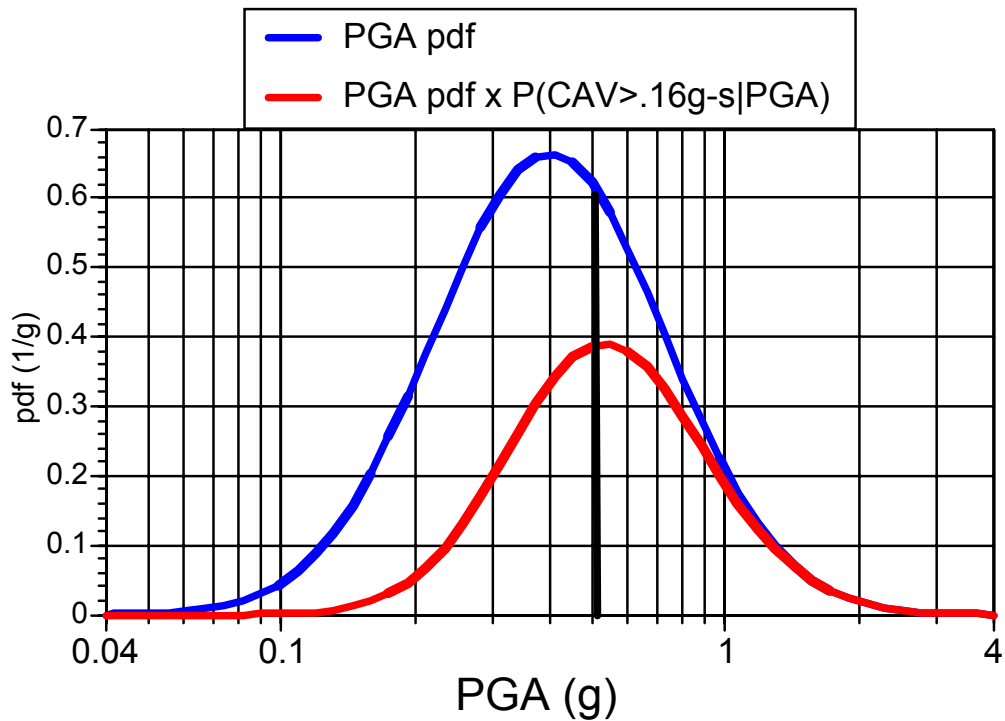


Figure 1-4
 Comparison of the PDF for PGA (Blue Curve) and the PGA PDF Scaled by the Probability of CAV>0.16g-s (Red Curve)

Accounting for the dependence of the variability of CAV and Sa, the joint probability can be written either as:

$$P(Sa > z, CAV > CAV_{\min} | M, R) = P(CAV > CAV_{\min} | M, R) P(Sa > z | CAV > CAV_{\min}, M, R)$$

Equation 1-5

or as:

$$P(Sa > z, CAV > CAV_{\min} | M, R) = P(Sa > z | M, R) P(CAV > CAV_{\min} | Sa > z, M, R)$$

Equation 1-6

If we use Equation 1-5, then we need to develop a model of CAV that depends on M and R and then develop a ground motion model that depends on M, R and CAV. Since the current ground motion models are not dependent on CAV, using this approach would require developing new ground motion models in addition to developing a CAV model. Alternatively, if we use Equation 1-6, then the ground motion model remains the same and we need to develop a CAV model that depends on M, R, and the Sa value.

To avoid having to develop new ground motion models, we use Equation 1-6. As a result, the CAV model must include the ground motion level, as well as other earthquake and site parameters. With this approach, the hazard integral becomes:

$$v(Sa > z, CAV > CAV_{\min}) = \sum_{i=1}^{N_{source}} N_i(M > M_{\min}) \int_{M_{\min}}^{M_{\max i}} \int_{r=0}^{\infty} f_{mi}(M) f_{ri}(r, M) P(Sa > z, | M, R) P(CAV > CAV_{\min} | Sa > z, M, r) dr dM$$

Equation 1-7

This form of the hazard integral has an implicit integration over the ground motion variability. This hazard integral can be re-written to explicitly integrate over the ground motion variability:

$$v(Sa > z, CAV > CAV_{\min}) = \sum_{i=1}^{N_{source}} N_i(M > M_{\min}) \int_{M_{\min}}^{M_{\max i}} \int_{r=0}^{\infty} \int_{\varepsilon} f_{mi}(M) f_{ri}(r, M) P(Sa > z, | M, R, \varepsilon) P(CAV > CAV_{\min} | Sa(M, R, \varepsilon), M, r) d\varepsilon dr dM$$

Equation 1-8

where ε is the number of standard deviations of the ground motion. The advantage of this form is that the CAV model is dependent on the Sa value rather than $Sa > z$. It is easier to develop a model for CAV given Sa, than it is to develop a model for CAV given $Sa > z$.

In this report, we develop models for estimating the CAV and show how to use the CAV model to remove earthquakes that are not potentially damaging from the hazard analysis. The NRC sent 15 Requests for Technical Update on this subject (Combined NRC RAI Comments on EPRI

Report 1012965 “Use of CAV in Determining Effects of Small Magnitude Earthquakes on Seismic Hazard Analyses”). These 15 RAIs, together with Industry responses to these RAIs, are contained within Appendix A of this report.

2

EMPIRICAL MODEL OF CAV

In this section, we derive empirical models for the CAV. Two approaches are used. In the first approach, we use the extensive WUS strong motion data set to derive models for CAV in two steps and we then check the applicability of these WUS based CAV models against strong motion data from CEUS/Canadian earthquakes. In the second approach, we use a combined data set of WUS and CEUS/Canadian ground motions to derive the CAV model in a single step and again check the resulting model against the CEUS/Canadian data by itself.

Empirical Data Set for WUS

The PEER NGA data set (PEER 2005) consists of 3551 recordings (mostly 3-component) from 173 earthquakes in active shallow crustal regions of the world. From this full dataset, recordings from individual earthquakes and recording stations were removed if the data were considered to be unreliable or not applicable to the WUS. In addition, components with $PGA < 0.025g$ were removed since these have zero CAV by definition. The resulting data set consists of 4,422 horizontal components from 97 earthquakes. The WUS data set used for developing the CAV model is given in the file “CAV_WUS_DATA_V2.XLS” which is included on the CD as noted in Appendix B.

The distribution of the earthquake moment magnitudes and rupture distances from the subset of WUS data used to develop the CAV model is shown in Figure 2-1. The data are primarily from earthquakes with moment magnitudes greater than 5.0. The distribution of the average shear-wave velocity in the top 30 m, V_{S30} , is shown in Figure 2-2. This figure shows that only a small fraction of the recordings are for hard rock conditions (e.g., $V_{S30} > 1500$ m/s) that are typically used for the EUS rock sites.

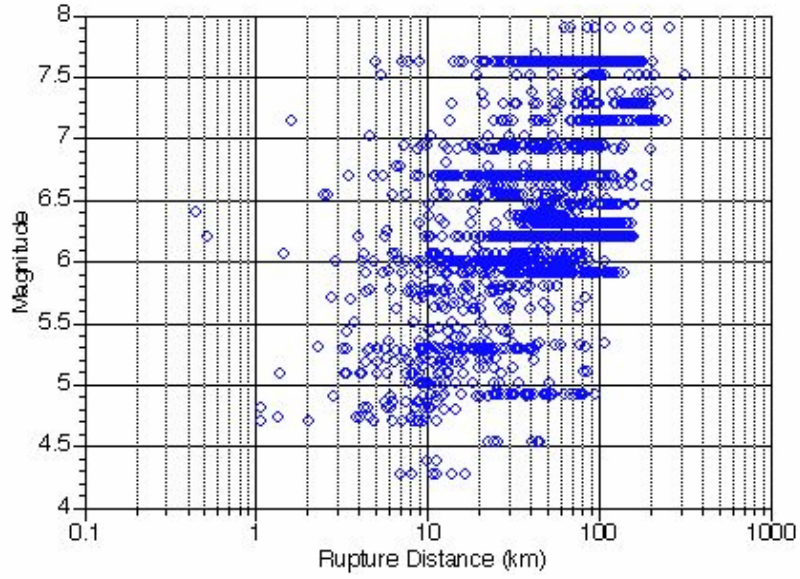


Figure 2-1
Distribution of Earthquake Magnitudes and Distances for the WUS Data Set

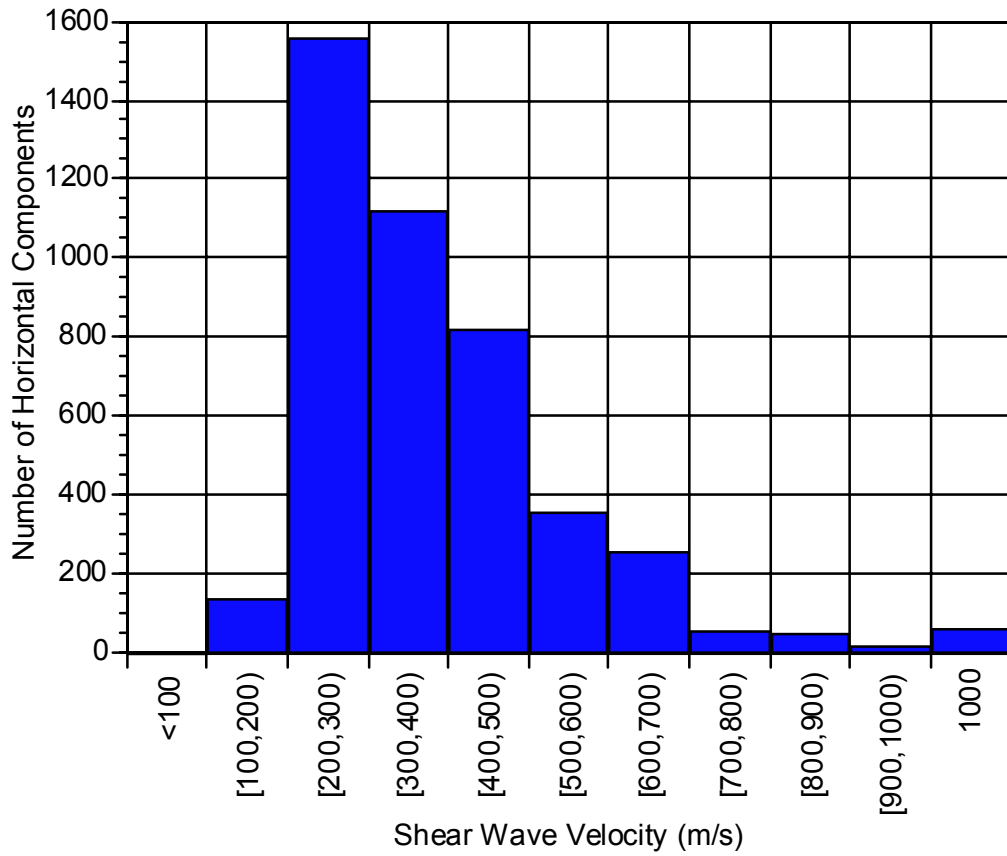


Figure 2-2
Distribution of V_{S30} Values for the WUS Data Set

Empirical Data Set for EUS

There are few strong motion data from CEUS earthquakes. EPRI (1993) compiled a list of ground motions recorded by CEUS and Canadian earthquakes through 1991. The earthquakes with $M \geq 4$ from the EPRI (1993) study are listed in Table 2-1. Note that earthquakes from Nahanni (northwest Canada) are included in Table 2-1. The ground motions from the Nahanni earthquakes have similar high frequency content as CEUS earthquakes so they are included as being representative of CEUS earthquakes. In addition to the data from EPRI (1993), the strong motion data from the 2005 Riviere-du-Loup, Quebec earthquake are also included (Table 2-1). Only 10 of the 17 CEUS/Canadian earthquakes listed in Table 2-1 had at least one horizontal component of ground motions with a PGA greater than 0.025g. The individual recordings with horizontal PGAs greater than 0.025g are listed in Table 2-2. Some of the records listed in Table 2-2 were not used in this study because the acceleration time series were not readily available for those stations. The CEUS/Canadian ground motion data used in this study is given in the file “CAV_EUS_DATA_V2.XLS” which is included on the CD as noted in Appendix B.

**Table 2-1
CEUS and Canadian Earthquakes with $M \geq 4$ from the EPRI (1993) Strong Motion Data Set
with at Least One Horizontal Component with $PGA > 0.025g$.**

EQID	Earthquake Name	Date	Hr	Min	Sec	M	m_{Lg}	No. of Horizontal Components with $PGA > 0.025g$
EPRI (1993)								
FK820100	Franklin Falls, New Hampshire	1982.01.19	0	14	42.00	4.3	4.8	12
NB820300	New Brunswick (A13)	1982.03.31	21	2	20.40	4.0	4.8	12
NH851100	Nahanni, Canada (F1)	1985.11.09	4	46		4.6		2
NH851200	Nahanni, Canada	1985.12.23	5	16	6.00	6.7		6
NH851201	Nahanni, Canada (A1)	1985.12.25	15	42		5.0		2
NO860100	Northeastern Ohio	1986.01.31	16	46	42.3	4.6	5.0	2
SG881101	Saguenay, Canada	1988.11.25	23	46	4.50	5.9	6.5	17
NM910501	New Madrid	1991.05.04	1	18	54.60	4.4	4.7	2
Additional Earthquakes								
RL050306	Riviere-du-Loup, Quebec	2005.03.06				4.8		7

Table 2-2
CEUS/CANADIAN Ground Motions with at Least One Horizontal Component with
PGA>0.0.25g

EPRI EQID	M	Station Name	Station Num	Distance (km)	Vs30 (m/s)	Comp H1	Comp H2	PGA H1 (g)	PGA H2 (g)
FK820100	4.3	Franklin Falls Dam Downstream	2627A	8	350	225	135	0.144	0.385
FK820100	4.3	Franklin Falls Dam Abutment	2627B	8	600	045	315	0.294	0.551
FK820100	4.3	Union Village Dam Downstream	2632C	62	600	245	155	0.038	0.016
FK820100	4.3	White River Junction VA Hospital	2604	61	1500	270	180	0.015	0.032
FK820100	4.3	North Springfield Dam Downstream	2630B	76	1500	275	185	0.032	0.023
NB820300	4.0	Homes Lake	HL	6	600	018	288	0.148	0.176
NB820300	4.0	Mitchell Lake Rd	MR	4	2000	028	118	0.204	0.137
NB820300	4.0	Loggie Lodge	LL	6	600	099	189	0.336	0.166
NB820300	4.0	Indian Brook	IB	3	600	231	321	0.334	0.273
NH851100	4.6	Site 2	6098	6	660	240	330	0.460	0.382
NH851200	6.76	Site 1	6097	10	660	010	280	0.978	1.096
NH851200	6.76	Site 2	6098	5	660	330	240	0.323	0.489
NH851200	6.76	Site 3	6099	5	660	360	270	0.139	0.148
NH851201	5.0	Site 3	6099	18	660	270	360	0.089	0.105
NO860100	4.6	PPBF		17	200	180	270	0.180	0.100
SG881101	5.9	St-Ferreol	GSC1	118	2000	000	270	0.121	0.097
SG881101	5.9	Quebec	GSC2	167	2000	051	321	0.051	0.051
SG881101	5.9	Tadoussac	GSC5	113	2000	097	007	0.027	-
SG881101	5.9	La Malbaie	GSC8	98	2000	063	333	0.124	0.060
SG881101	5.9	St-Pascal	GSC9	132	2000	000	270	0.046	0.056
SG881101	5.9	Riviere-Quelle	GSC10	118	2000	000	270	0.040	0.057
SG881101	5.9	Chicoutimi	GSC16	52	2000	214	124	0.107	0.131
SG881101	5.9	St-Andre-du-lac	GSC17	70	2000	000	270	0.156	0.091
SG881101	5.9	Les Eboulements	GSC20	95	2000	000	270	0.125	0.102
RL050306	4.8	A16		41	1500	000	090	0.021	0.034
RL050306	4.8	A21		19	1500	000	090	0.070	0.075
RL050306	4.8	A61		33	1500	000	090	0.057	0.071
RL050306	4.8	A64		23	1500	000	090	0.023	0.033
RL050306	4.8	LMQ		53	1500	000	090	0.018	0.028

Model for CAV Based on WUS Data – 2-Step Approach

Given the definition of CAV shown in Equation 1-2, CAV will depend on the average acceleration and the duration of shaking. The CAV values from the WUS data set are shown in Figure 2-3 as a function of the PGA and in Figure 2-4 as a function of duration. For the duration, we use the uniform duration defined by Bolt (1973) as the total time during which the absolute value of the acceleration time series exceeds a specified threshold. Since the CAV is only measured for PGA values $>0.025g$, we have used a threshold of $0.025g$ for the uniform duration. Comparing Figures 2-3 and 2-4, the variability of CAV as a function of uniform duration is much less than the variability of CAV as a function of the PGA.

While the uniform duration is not directly available from the PSHA results, we chose to model CAV as a function of the uniform duration (and other secondary factors), and then model the dependence of the duration on other parameters such as PGA, magnitude, and V_{S30} because this provides a simple physical aspect of ground motion that can be modified for CEUS conditions. This approach allows the CAV model to be modified for CEUS conditions, if needed, based on differences in the duration in the WUS and CEUS.

There are two steps in the development of the CAV model: (1) develop a CAV model based on duration, and (2) develop a duration model based on earthquake and site parameters. The models can then be combined to give a CAV model based on earthquake and site parameters. The models developed in these two steps are described below.

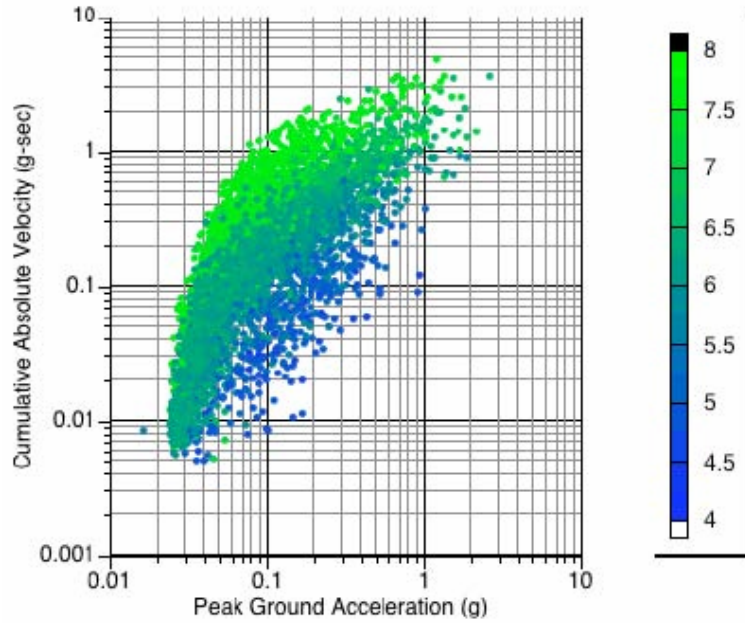


Figure 2-3
Dependence of the CAV on the PGA and Magnitude

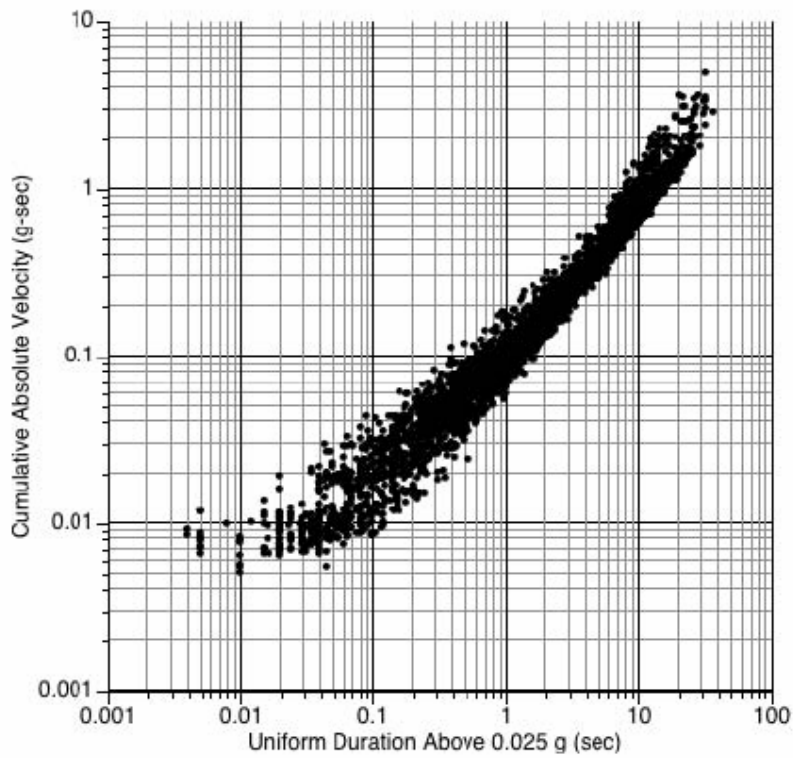


Figure 2-4
Duration Dependence of the CAV

Step 1 – Model for CAV Including Duration Dependence

Based on the plot of the CAV values in Figure 2-4, CAV is approximately lognormally distributed and is heteroscedastic (non-constant standard deviation) with the standard deviation decreasing with increasing duration. The standard deviation becomes large for smaller durations (e.g., duration <0.2 sec), but this range of ground motions is not important for determining if the CAV exceeds the 0.16g-sec threshold.

The data shown in Figure 2-4 indicate that there is some curvature in the $\ln(\text{CAV})$ as a function of the $\ln(\text{duration})$. Therefore, an initial CAV model was developed based on a quadratic function of $\ln(\text{duration})$:

$$\ln(\text{CAV}) = a_1 + a_2 \ln(\text{Dur}_{uni}) + a_3 (\ln(\text{Dur}_{uni}))^2 \quad \text{Equation 2-1}$$

Figures 2-5, 2-6, and 2-7 show the CAV residuals from this initial CAV model as a function of M , PGA , and V_{S30} , respectively. The residuals with magnitude (Figure 2-5) show a trend with an increasing slope for the smaller magnitudes. A quadratic function of magnitude is needed to model this dependence. The residual with PGA (Figure 2-6) show strong curvature. To model this strong curvature, a fourth order polynomial of $\ln(\text{PGA})$ is needed. To avoid unconstrained behavior of the model for PGA values beyond the data range (about 1.5 g), the PGA dependence was limited to extrapolation of the linear term with $\ln(\text{PGA})$ for PGA values greater than 1g. The residuals with V_{S30} do not show a trend, but a linear dependence on $\ln(V_{S30})$ was added to accommodate a possible small effect.

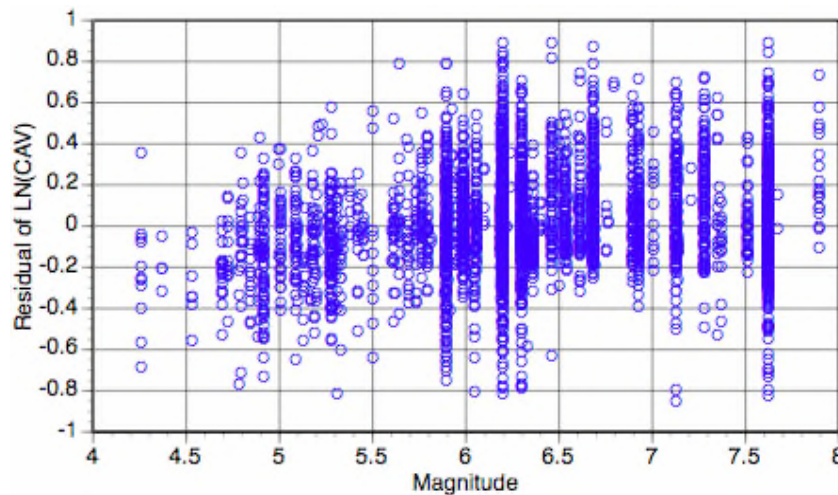


Figure 2-5
Residuals of Initial CAV Model (Equation 2-1) as a Function of Magnitude

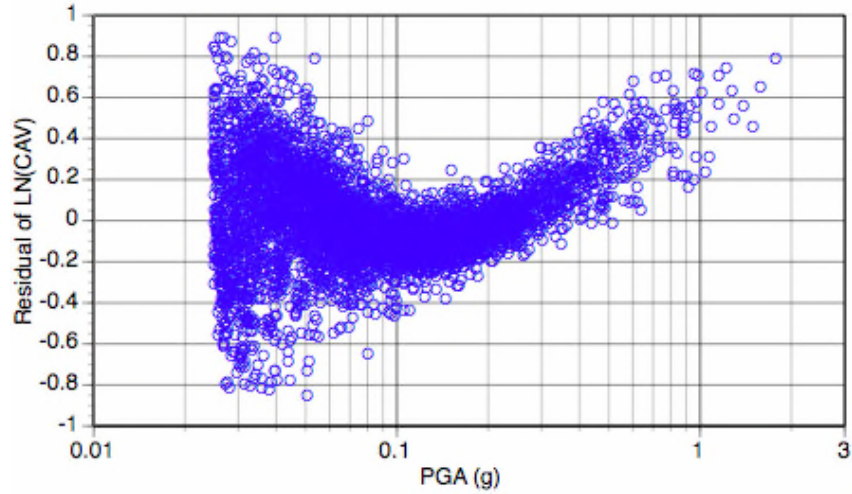


Figure 2-6
Residuals of Initial CAV Model (Equation 2-1) as a Function of PGA

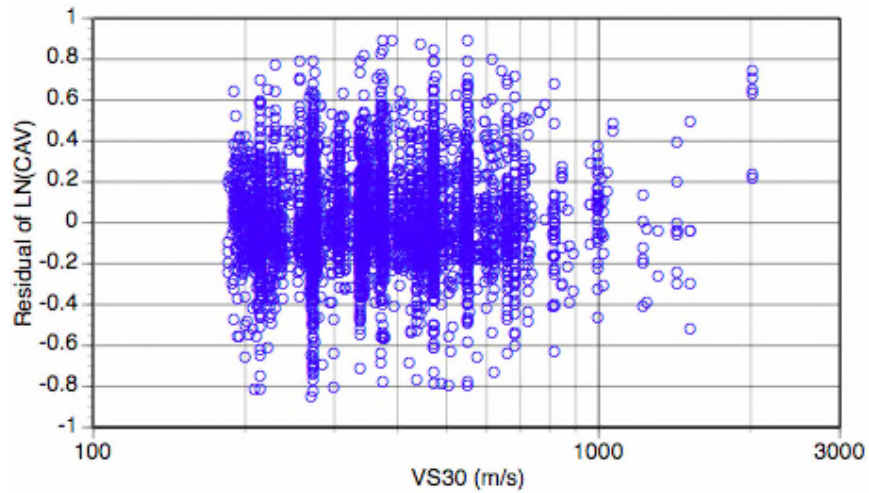


Figure 2-7
Residuals of Initial CAV Model (Equation 2-1) as a Function of V_{S30}

Based on this evaluation of the residuals of the initial model, the CAV is modeled as a function of uniform duration, PGA, M , and V_{S30} using the following functional form:

$$\ln(CAV(g-s)) = \begin{cases} c_0 + c_1(M - 6.5) + c_2(M - 6.5)^2 + c_3 \ln(PGA) \\ + c_4(\ln(PGA))^2 + c_5(\ln(PGA))^3 + c_6(\ln(PGA))^4 \\ + c_7(\ln(V_{S30}) - 6) + c_8 \ln(Dur_{umi}) + c_9(\ln(Dur_{umi}))^2 & \text{for } PGA \leq 1g \\ c_0 + c_1(M - 6.5) + c_2(M - 6.5)^2 + c_3 \ln(PGA) \\ + c_7(\ln(V_{S30}) - 6) + c_8 \ln(Dur_{umi}) + c_9(\ln(Dur_{umi}))^2 & \text{for } PGA > 1g \end{cases}$$

Equation 2-2

where M is the moment magnitude, Dur_{uni} is the uniform duration above 0.025g in sec, PGA is the peak horizontal acceleration in g, and the V_{S30} is the shear-wave velocity over the top 30m in m/s.

A regression analysis was performed using ordinary least-squares to estimate the coefficients in Equation 2-2. The resulting coefficients are listed in Table 2-4. The asymptotic standard errors of the estimates are also listed in parentheses. Based on the asymptotic standard errors, the C_3 term (linear dependence on $\ln(PGA)$) is not statistically significant and the C_7 term (dependence on $\ln(V_{S30})$) is marginally significant. These terms could be removed from the model with a negligible change to the model.

The median CAV model is shown in Figures 2-8 and 2-9. These figures show that the CAV is only weakly dependent on PGA, magnitude, and V_{S30} if the duration is known. The standard deviation ranges from 0.37 for small duration to 0.10 natural log units for large durations, which is very small for ground motion models indicating that CAV is well determined if the duration, PGA, M , and V_{S30} are known.

The residuals* of the CAV model are shown as a function of duration, PGA, magnitude, and V_{S30} in Figures 2-10, 2-11, 2-12, and 2-13 respectively. Figure 2-10 shows a strong trend in the residuals for very small duration values (less than 0.04 sec), but these values are well below the threshold of interest so this trend is not relevant. The other three figures do not show any significant trends in the residuals.

Table 2-3
Coefficients for CAV Model

Coefficient	Estimate (Standard Error)
C_0	-1.75 (0.04)
C_1	0.0567 (0.0062)
C_2	-0.0417 (0.0043)
C_3	0.0737 (0.10)
C_4	-0.481 (0.096)
C_5	-0.242 (0.036)
C_6	-0.0316 (0.0046)
C_7	-0.00936 (0.00833)
C_8	0.782 (0.006)
C_9	0.0343 (0.0013)
$\sigma_{\ln CAV1}$	$\begin{cases} 0.37 & \text{for } Dur_{uni} < 0.2 \\ 0.37 - 0.090(\ln(Dur_{uni}) - \ln(0.2)) & \text{for } 0.2 \leq Dur_{uni} \leq 4 \\ 0.10 & \text{for } Dur_{uni} > 4 \end{cases}$

* Residuals are estimates of experimental error obtained by subtracting the observed responses from the predicted responses.

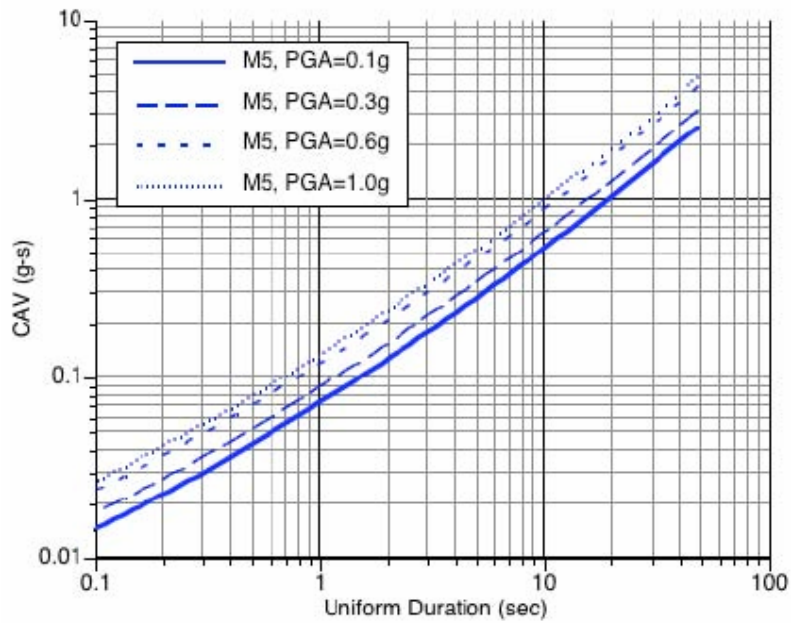


Figure 2-8
Median CAV Model for $V_s=600\text{m/s}$ for Different PGA Values

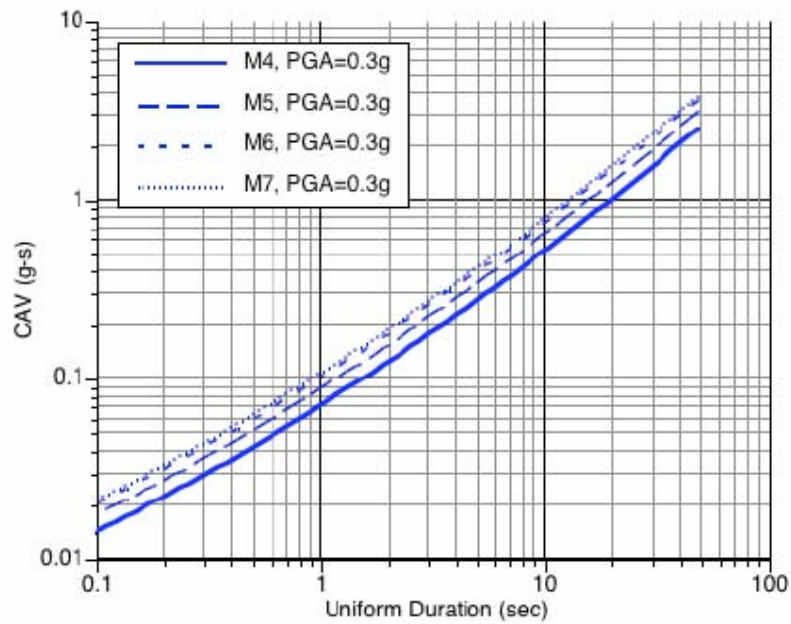


Figure 2-9
Median CAV Model for $V_s=600\text{m/s}$ for Different Magnitudes

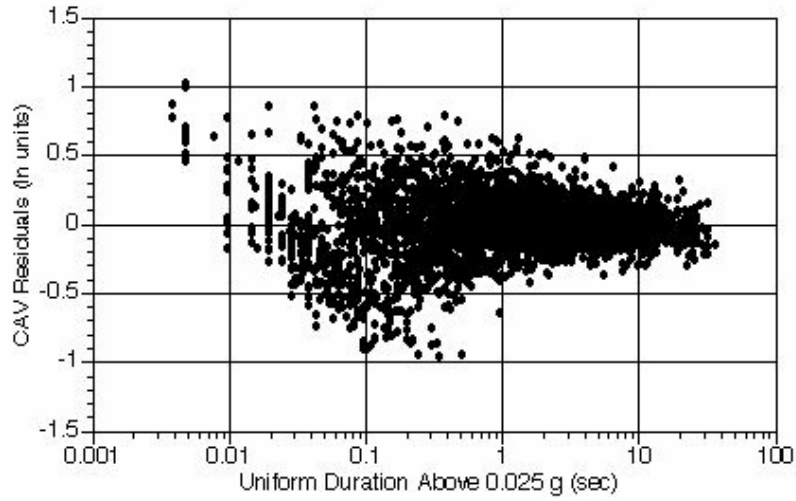


Figure 2-10
Duration Dependence of the CAV Residuals

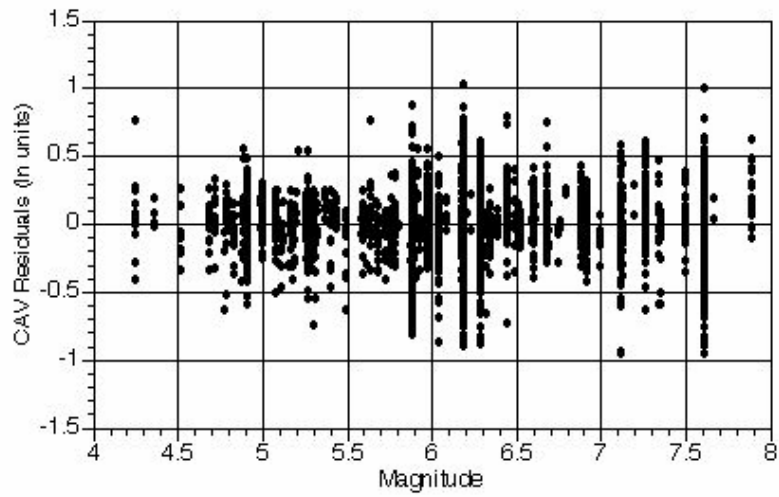


Figure 2-11
Magnitude Dependence of the CAV Residuals

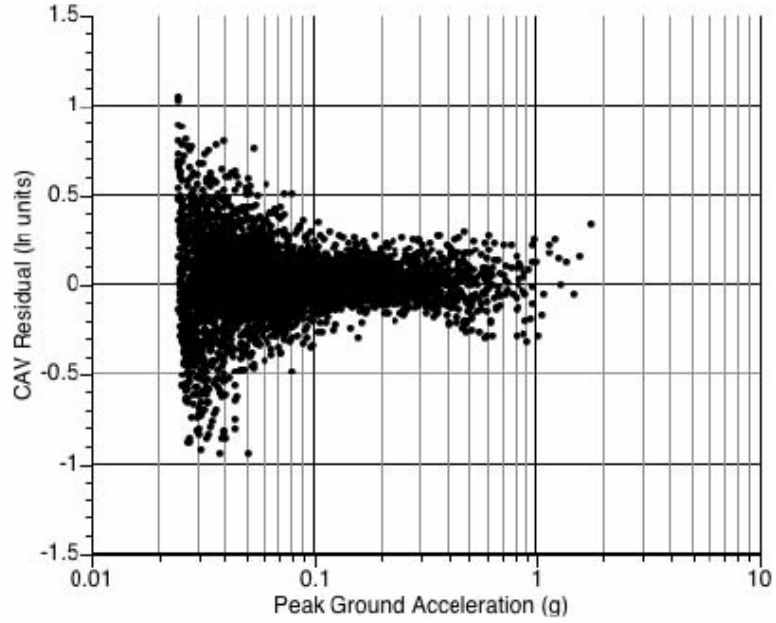


Figure 2-12
PGA Dependence of the CAV Residual

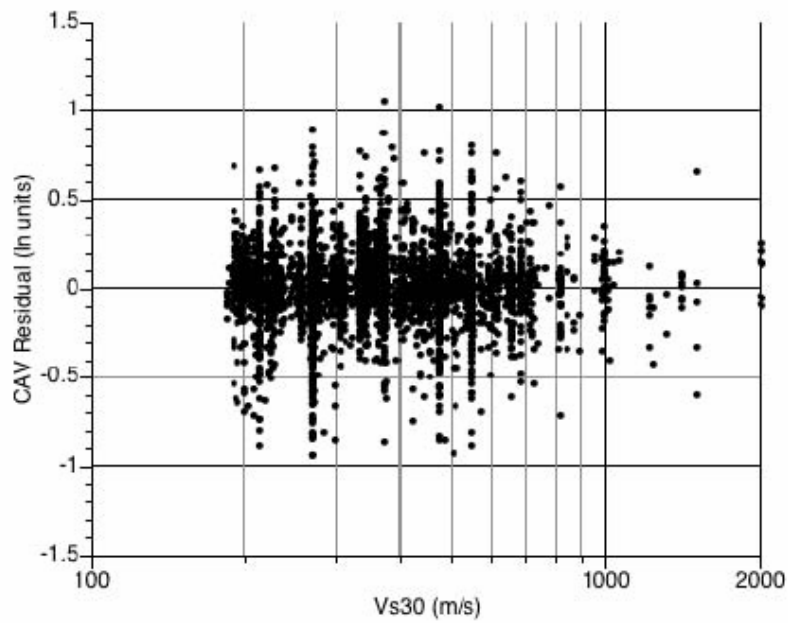


Figure 2-13
 V_{s30} Dependence of the CAV Residual

Using this WUS based CAV model, we then computed the residuals for ground motions from CEUS and Canadian earthquakes. The residuals, shown in Figure 2-14 as a function of the PGA, do not show a significant bias and show that the variability is increased for small PGA near the 0.025g threshold. These residuals indicate that the WUS CAV model is applicable to the EUS if the uniform duration of the CEUS data is known. Later, we test if the uniform durations for the CEUS and Canadian earthquakes are significantly from that of the WUS earthquakes.

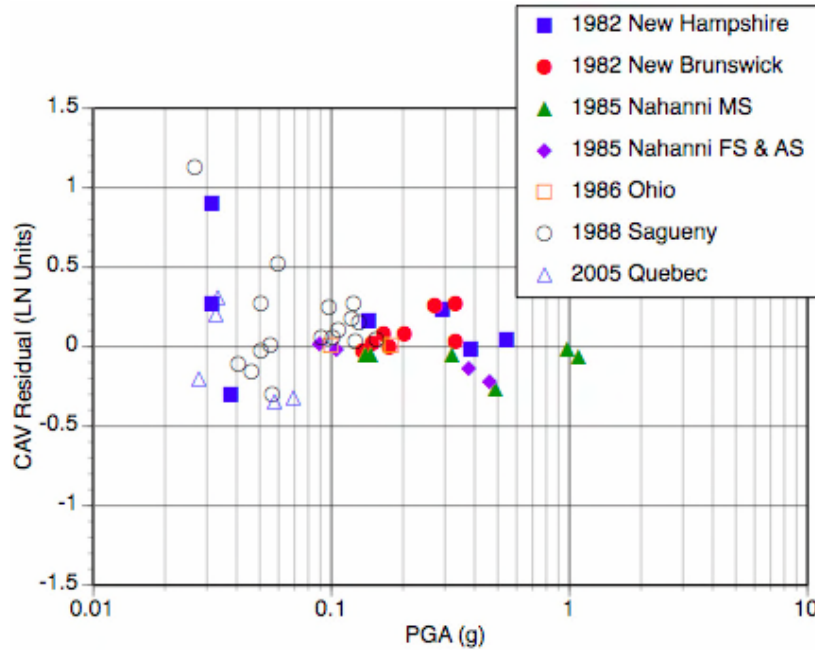


Figure 2-14
CAV Residuals for CEUS/Canadian Data Using the Observed Uniform Durations

Step 2 – Model for Uniform Duration

The CAV model derived in step 1 includes uniform duration as a parameter. To use the model to compute the conditional probability of CAV>0.16g-s for a given M, R, V_{S30}, and PGA for use in the PSHA, we need to develop a model to estimate uniform duration as a function of M, R, V_{S30}, and PGA. In this step, we develop a model for uniform duration above 0.025g using the same WUS data set used to develop the CAV model.

The uniform duration is shown as a function of magnitude and PGA in Figure 2-15 and 2-16. Comparing Figures 2-15 and 2-16, the uniform duration is more strongly correlated with PGA than with magnitude. The ln(Dur_{uni}) falls off rapidly as the PGA approaches 0.025g. To capture this dependence, we used the following initial model:

$$\ln(Dur_{uni}(s)) = a_1 + a_2 \ln(PGA) + \frac{a_3}{\ln(PGA) + a_4} \tag{Equation 2-3}$$

The residuals of the duration from this initial model are shown as functions of M, VS30, and distance in Figures 2-17, 2-18, and 2-19, respectively. There is a strong trend in the residuals

with magnitude with a change in slope above magnitude 6 indicating that a quadratic magnitude dependence is needed. There is a weak trend with distance, but since magnitude and distance are partially correlated in the data set, we chose to model the magnitude dependence first and then check the distance dependence of the resulting residuals. There is a weak trend in the residuals as a function of the VS30 and since the VS30 is not strongly correlated with magnitude, we allowed for this trend by adding a linear $\ln(\text{VS30})$ term to the model.

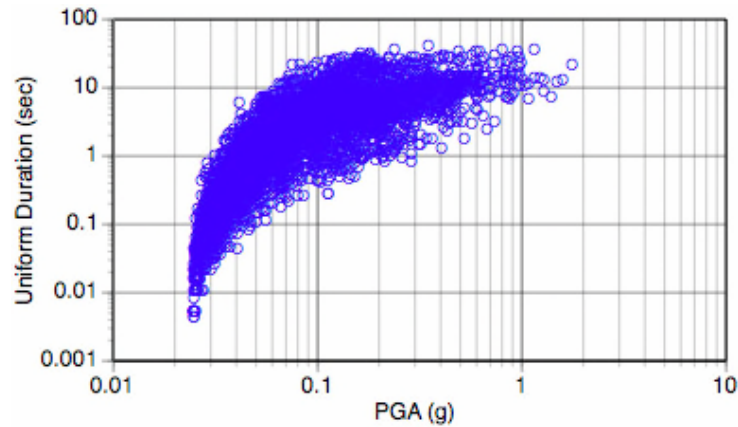


Figure 2-15
Dependence of the Uniform Duration with PGA

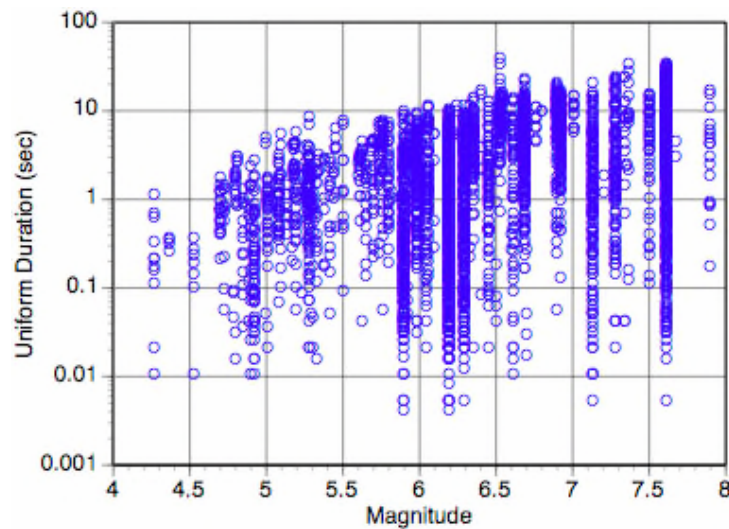


Figure 2-16
Dependence of the Uniform Duration with Magnitude

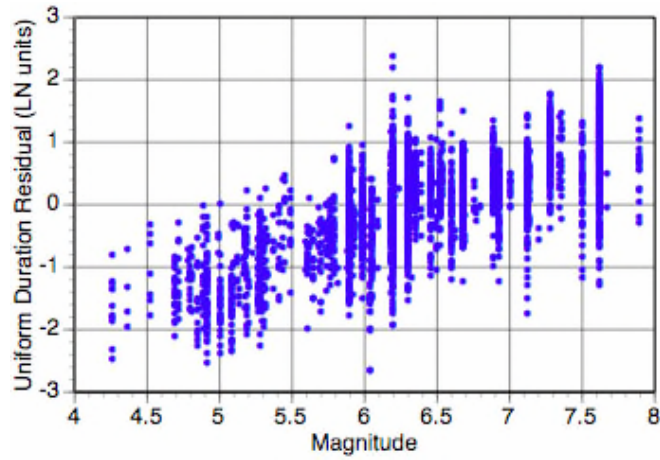


Figure 2-17
Magnitude Dependence of the Residuals of the Uniform Duration from the Initial Model for WUS Data

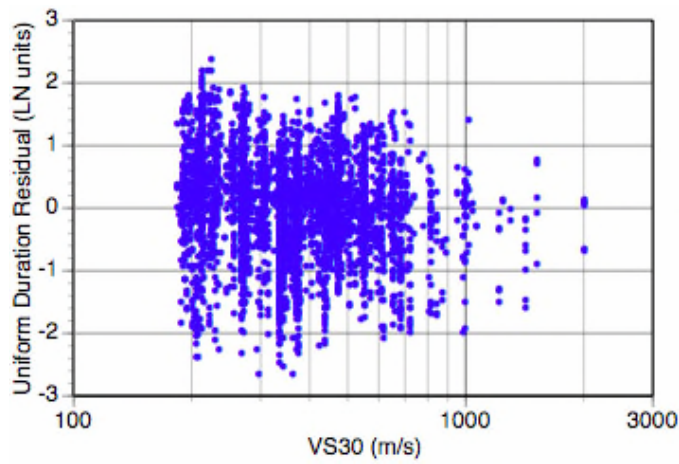


Figure 2-18
 V_{S30} Dependence of the Residuals of the Uniform Duration from the Initial Model for WUS Data

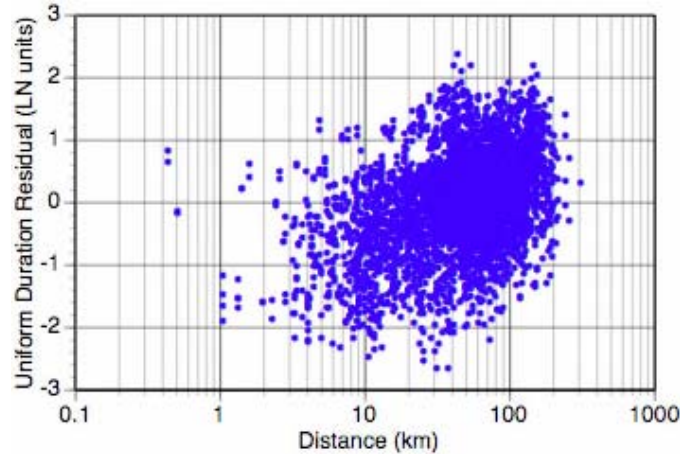


Figure 2-19
Distance Dependence of the Residuals of the Uniform Duration from the Initial Model for WUS Data

Based on the evaluation of the residuals, the following functional form is used to model the uniform duration:

$$\ln(Dur_{uni}(s)) = a_1 + a_2 \ln(PGA) + \frac{a_3}{\ln(PGA) + a_4} + a_5(M - 6.5) + a_6(M - 6.5)^2 + a_7(\ln(V_{S30}) - 6)$$

Equation 2-4

The coefficients computed using ordinary least-squares are listed in Table 2-5. The standard deviation is 0.51 natural log units. Unlike the CAV model, the duration has a significant dependence on the V_{S30} with duration increasing for softer sites.

The resulting median duration is shown as a function of the PGA for different magnitudes in Figure 2-20. The residuals of the uniform duration model using the WUS data are shown in Figures 2-21, 2-22, 2-23, and 2-24 for PGA, magnitude, distance, and V_{S30} , respectively. These figures do not show any significant trends in the residuals. In particular, there is no trend in the residuals as a function of distance, so a distance term is not needed in the model.

Table 2-4
Coefficients for Uniform Duration Model

Coefficient (Eq. 2-4)	Estimate (Standard Error)
a_1	3.50 (0.05)
a_2	0.0714 (0.0421)
a_3	-4.19 (0.30)
a_4	4.28 (0.03)
a_5	0.733 (0.010)
a_6	-0.0871 (0.0105)
a_7	-0.355 (0.020)
$\sigma_{\ln DUR}$	0.509

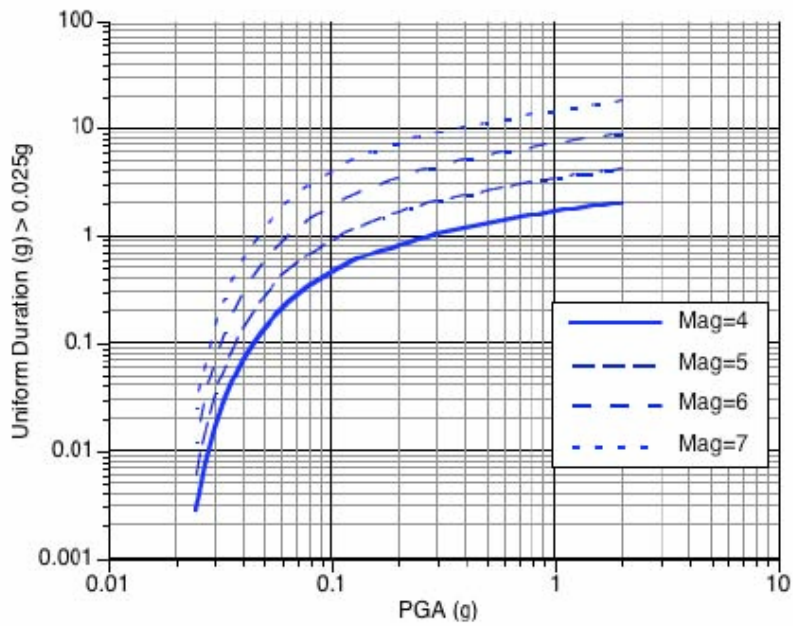


Figure 2-20
Median Uniform Duration for $V_{S30}=600$

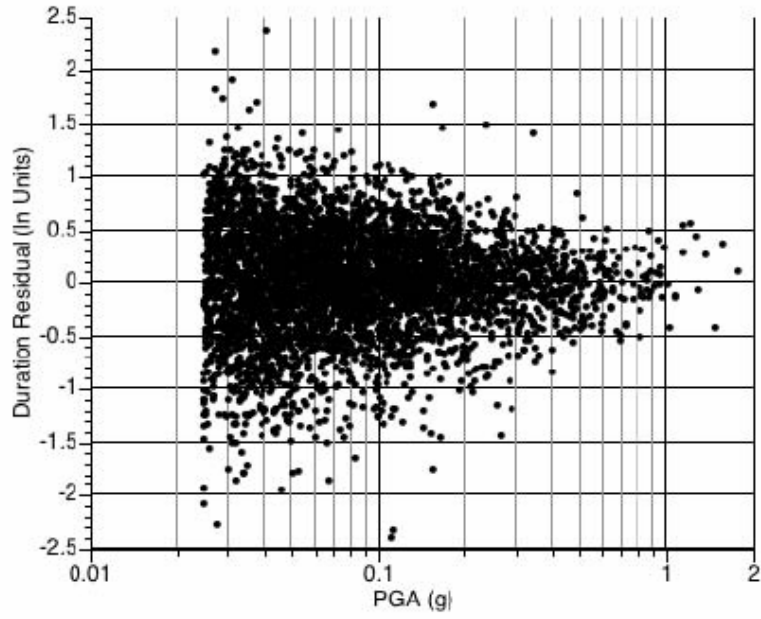


Figure 2-21
PGA Dependence of the Uniform Duration Residuals

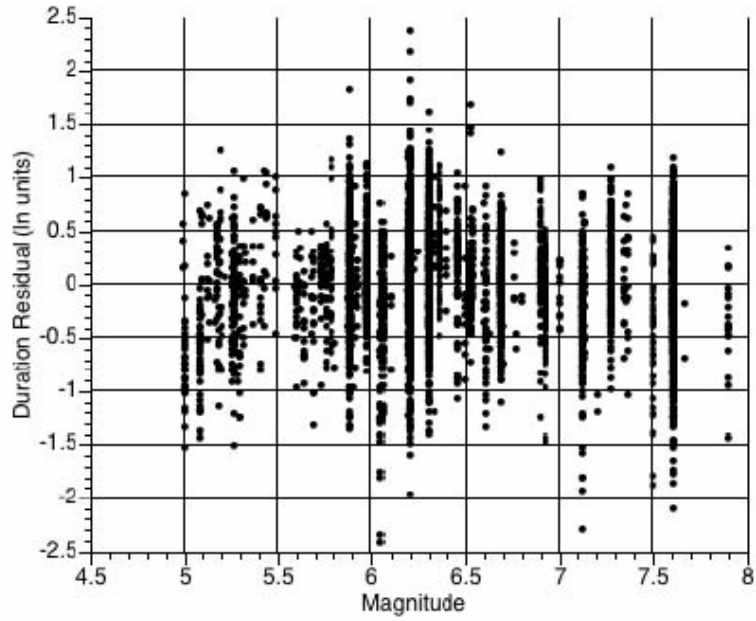


Figure 2-22
Magnitude Dependence of the Uniform Duration Residuals

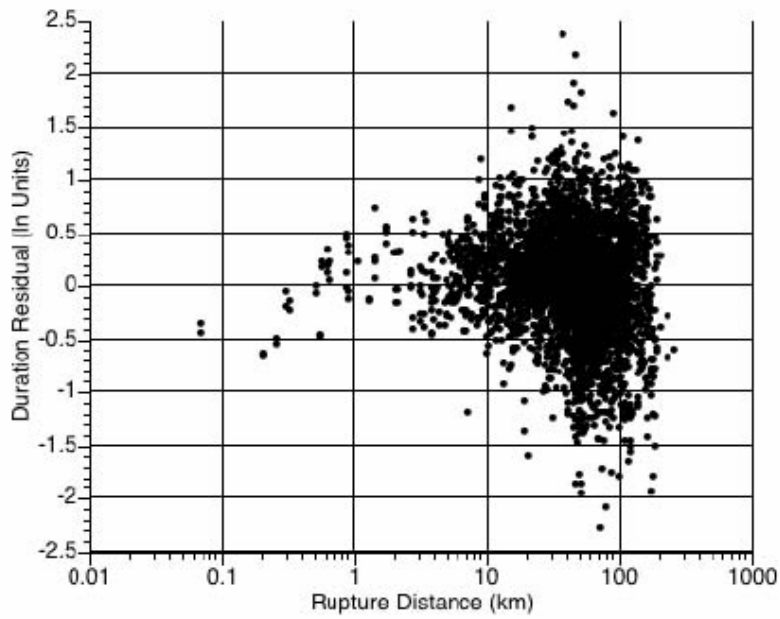


Figure 2-23
Distance Dependence of the Uniform Duration Residuals

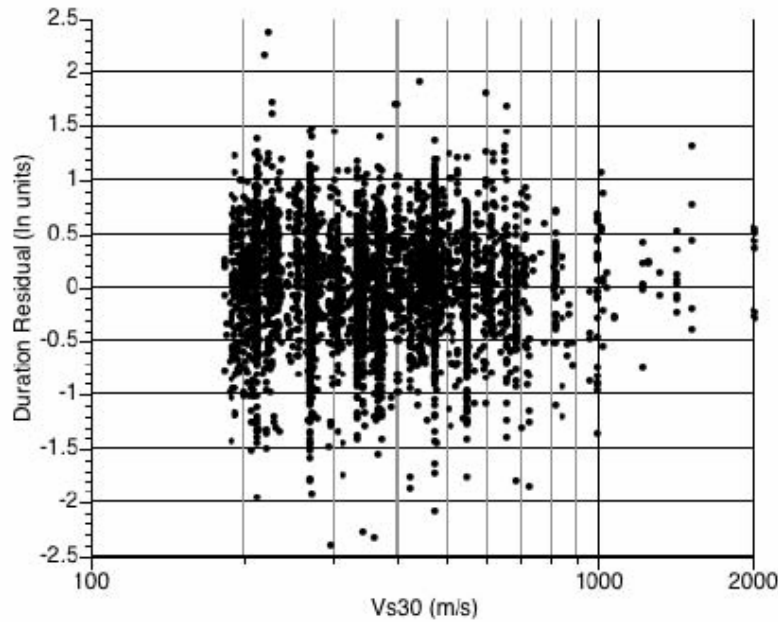


Figure 2-24
Shear-Wave Velocity Dependence of the Uniform Duration Residuals

Using the WUS based duration model, we then computed the duration residuals for CEUS/Canadian ground motions with PGA values greater than 0.025g. The duration residuals, shown in Figures 2-25, 2-26, and 2-27 as functions of the PGA, M , and V_{S30} indicate that there is slight trend in the residuals as a function of PGA with a bias toward negative residuals (over-prediction) for PGA values greater than 0.2g. Overall, the mean residual is 0.10 ± 0.09 which is not significantly different from zero. If the nine points with PGA values less than 0.05g are excluded as being too small to be relevant, then the bias is reduced to 0.04 ± 0.09 . Therefore, based on the available CEUS/Canadian data set, the WUS duration model is considered to be applicable to the CEUS.

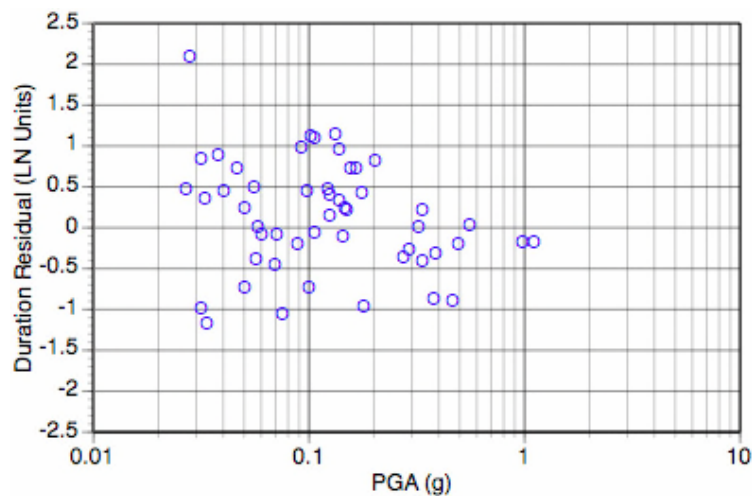


Figure 2-25
PGA Dependence of the Uniform Duration Residuals from the ENA Ground Motions Listed in Table 2-2

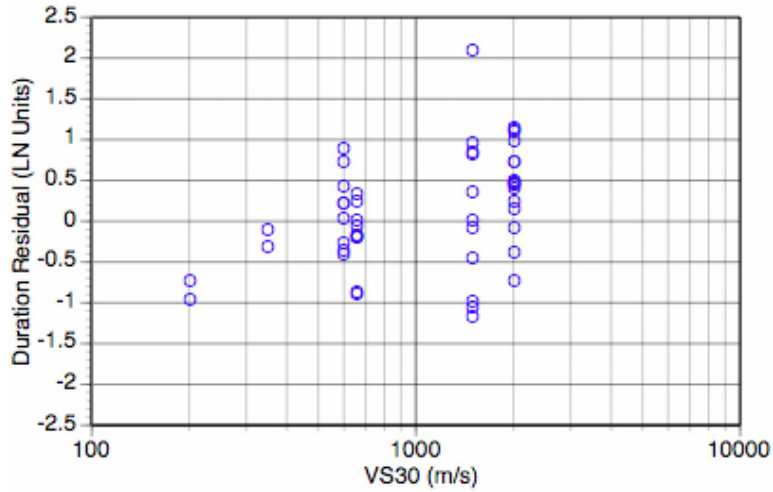


Figure 2-26
 V_{S30} Dependence of the Uniform Duration Residuals from the ENA Ground Motions Listed in Table 2-2

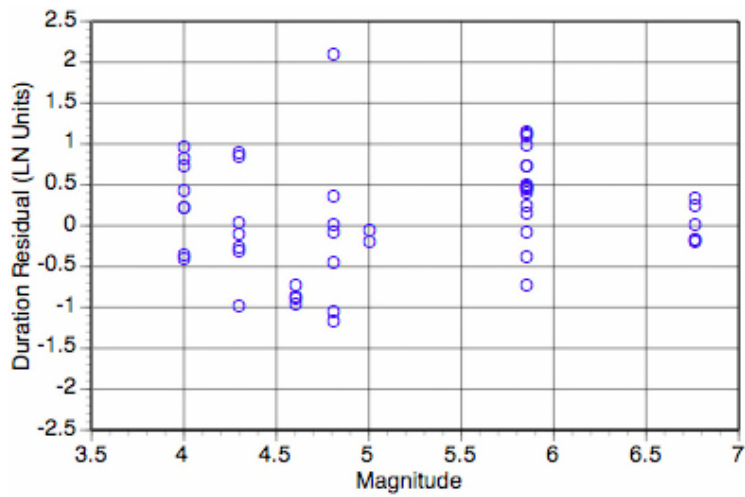


Figure 2-27
Magnitude Dependence of the Uniform Duration Residuals from the ENA Ground Motions Listed in Table 2-2

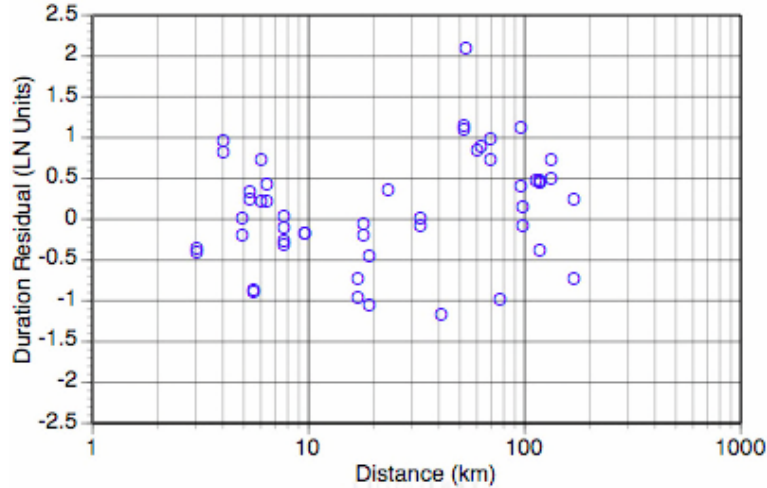


Figure 2-28
Distance Dependence of the Uniform Duration Residuals from the ENA Ground Motions Listed in Table 2-2

Combined Model for CAV

To apply the CAV model in a standard PSHA, the actual value of the duration will not be available; therefore, we need to use an estimate of the duration. For the previous section, we have a model for the median duration and also the standard deviation. The variability of the duration is high (0.51 natural log units) and we need to account for the effect of this variability on the variability of the CAV. If we estimate the duration using the median duration from Equation 2-4, we can compute the total variability of the CAV by standard propagation of errors:

$$\sigma_{\ln CAV} = \sqrt{\left(\frac{\partial \ln CAV}{\partial \ln Dur}\right)^2 \sigma_{\ln Dur}^2 + \sigma_{\ln CAV_1}^2 + \left(\frac{\partial \ln CAV}{\partial \ln Dur}\right) COV(\varepsilon_{\ln CAV}, \varepsilon_{\ln Dur})}$$

Equation 2-5

where $\sigma_{\ln CAV_1}$ is the standard deviation of the $\ln(CAV)$ model from Equation 2-2 (e.g., based on the observed durations). A check of the correlation of the residuals found that the COV is small (about 0.01) so the last term in Equation 2-4 can be dropped. Computing the partial derivative from Equation 2-2, the total standard deviation of the $\ln(CAV)$ model (given the PGA, M, and V_{s30}) is given by:

$$\sigma_{\ln CAV} = \sqrt{(c_8 + 2c_9 \ln(D\hat{u}_{uni}))^2 \sigma_{\ln dur}^2 + \sigma_{\ln CAV_1}^2}$$

Equation 2-6

The total standard deviation is shown in Figure 2-29 as a function of the median duration.

The residuals of EUS CAV computed using the median durations are shown in Figure 2-30 as a function of PGA. The mean residual is 0.12 ± 0.08 indicating a small under-prediction of the CAV. This bias is strongly dependent on the recordings with very small PGA values. If the values with PGA values less than 0.05g are excluded, then the bias is reduced to 0.05 ± 0.08 .

Since these small PGA values are not relevant to our intended application, we conclude that the WUS model is applicable to the CEUS. There is a trend that the model over-predicts the CAV values for PGA values greater than 0.2g. This indicates that using the WUS-based CAV model will over-predict the CAV values for larger PGA.

The residuals of the CAV based on this two-step method are shown in Figures 2-31, 2-32, and 2-33 as functions for magnitude, V_{S30} , and distance, respectively. In these figures, the data for PGA values less than 0.05g are shown in red. These residual plots show some trends with distance: over-prediction for distances 20-40 km and under-prediction for distances of 50-100 km.

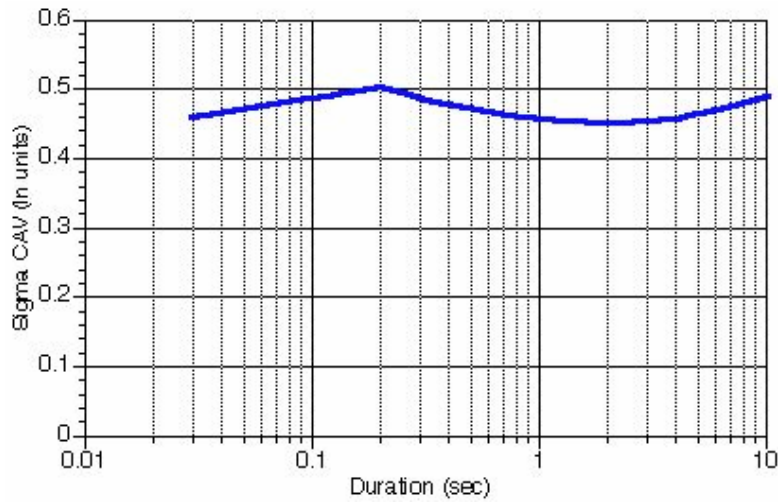


Figure 2-29
Standard Deviation of the $\ln(\text{CAV})$ if the Median Duration Model is Used

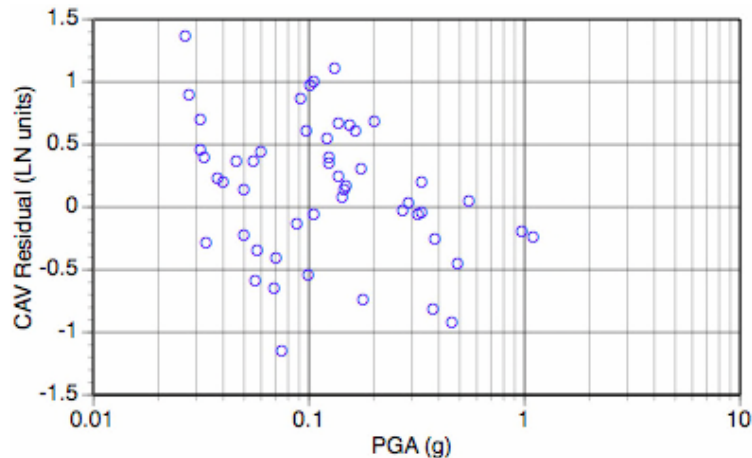


Figure 2-30
PGA Dependence of the ENA CAV Residuals Using the Median Duration

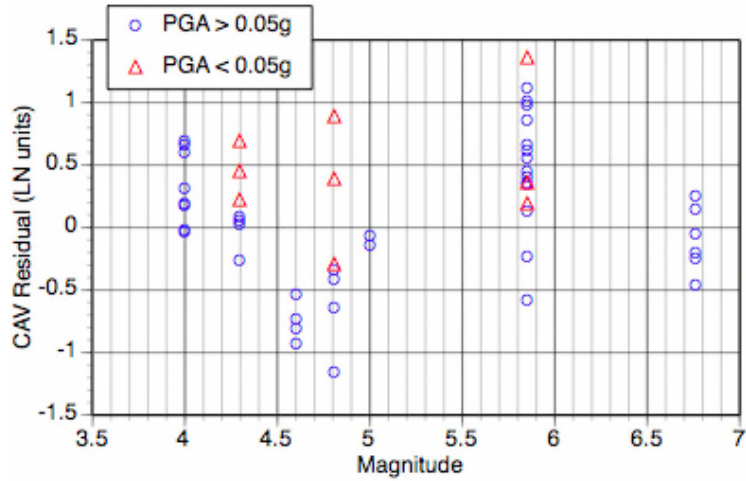


Figure 2-31
Magnitude Dependence of the ENA CAV Residuals Using the Median Duration

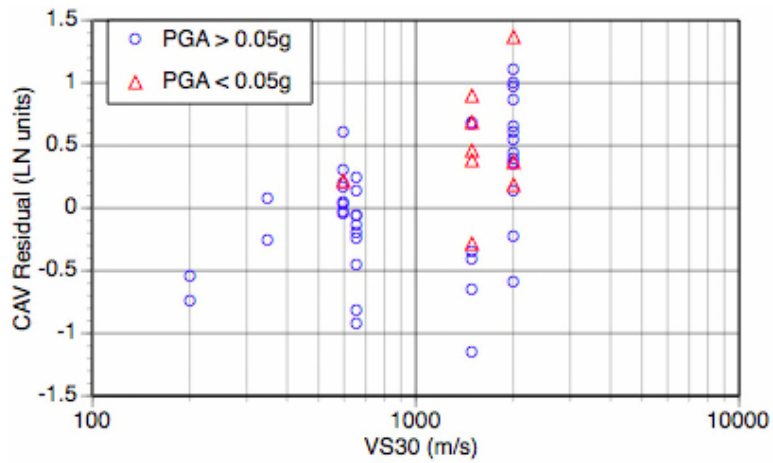


Figure 2-32
 V_{S30} Dependence of the ENA CAV Residuals Using the Median Duration

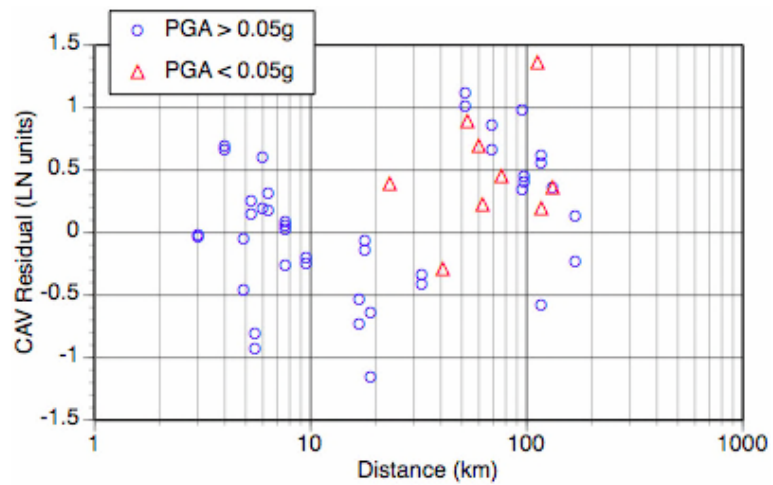


Figure 2-33
Distance Dependence of the ENA CAV Residuals Using the Median Duration

Probability of Exceeding Specified CAV Value

The probability of exceeding a CAV value of 0.16g-sec is given by:

$$P(CAV > 0.16g - s | PGA, M, V_{s30}) = \begin{cases} 1 - \Phi(\varepsilon_{CAV}^*) & \text{for } PGA \geq 0.025g \\ 0 & \text{for } PGA < 0.025g \end{cases} \quad \text{Equation 2-7}$$

where Φ is the cumulative normal distribution and ε_{CAV}^* is the number of standard deviations in the CAV model that will yield 0.16g-sec. That is,

$$\varepsilon_{CAV}^* = \frac{\ln(0.16) - \ln CAV(PGA, M, V_{s30}, \hat{D}_{ur}(PGA, M, V_{s30}))}{\sigma_{\ln CAV}} \quad \text{Equation 2-8}$$

where the CAV is given by Equation 2-2 and $\sigma_{\ln CAV}$ is given by Equation 2-5. The probability of exceeding a CAV value of 0.16 g-s is shown in Figure 2-34.

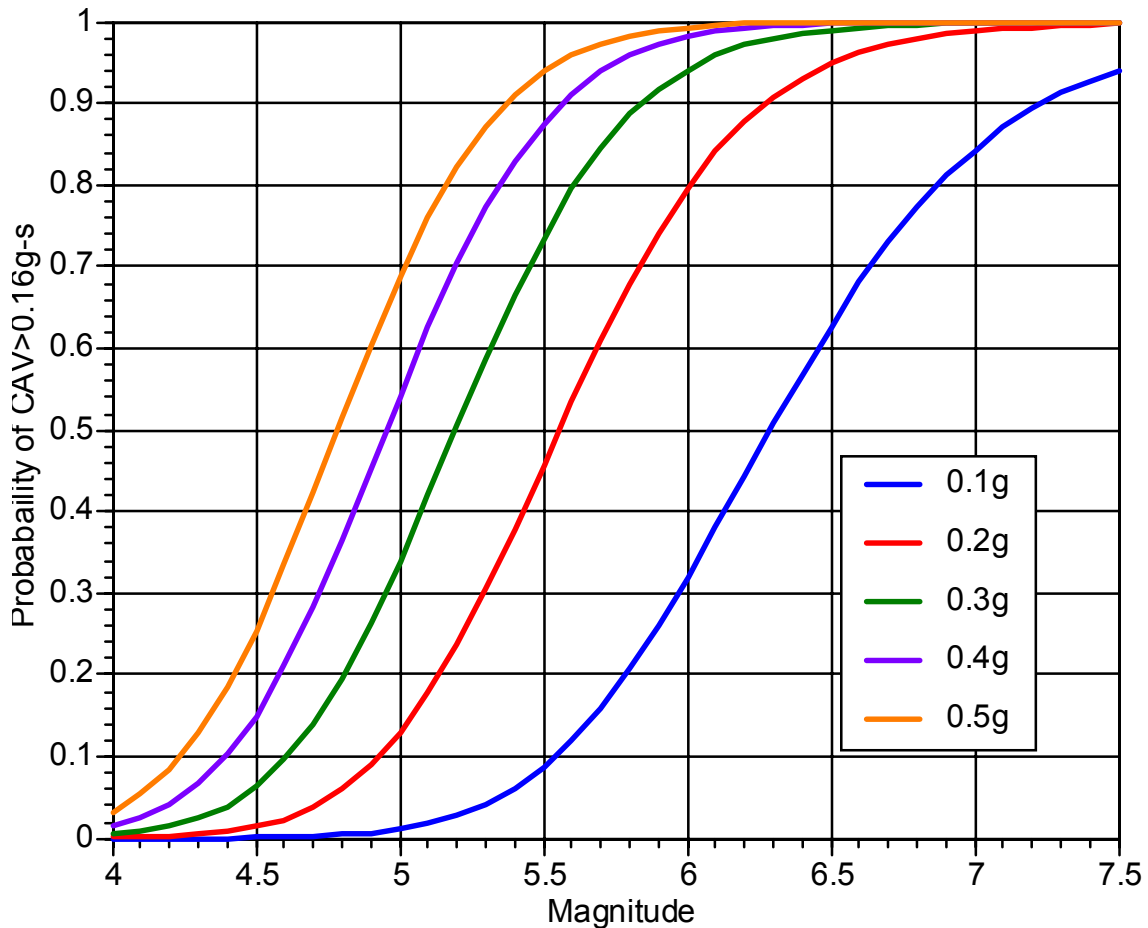


Figure 2-34
Probability of CAV>0.16g-sec for $V_s=1000m/s$ Using the Two-Step Approach

Model for CAV Based on Combined WUS/CEUS/Canadian Data – 1-Step Approach

The 2-step approach described in the previous section found that there was no need to modify the duration model for ENA earthquakes. Therefore, we can simplify the process to a single step in which we derive a model for the CAV without going through the duration. For this analysis, we used the combined WUS and ECUS/Canadian data sets. As discussed in Chapter 1, the CAV model must include the ground motion to account for the correlation of the variability of the CAV and the ground motion.

Since the scaling of CAV is similar to the scaling of the duration, we used an initial model that follows the form used for the duration (see Equation 2-4). This model is given by:

$$\ln(\text{CAV}(g-s)) = d_1 + d_2(\ln(\text{PGA}) + 2.5) + \frac{d_3}{\ln(\text{PGA}) + d_4} + d_5(M - 6.5) + d_6(M - 6.5)^2 + d_7(\ln(V_{S30}) - 6) \quad \text{Equation 2-9}$$

The resulting coefficients for this model are given in Table 2-5. The residuals for the single step model are shown in Figure 2-35, 2-36, 2-37, and 2-38 as functions of PGA, V_{S30} , magnitude, and distance, respectively.

The resulting probability of exceeding CAV for the single step model is compared to that from the two-step model in Figure 2-39 for $V_{S30}=1000\text{m/s}$. The two approaches lead to similar models.

Table 2-5
Coefficients for Single Step CAV Model

Coefficient (Equation 2-9)	Estimate (Standard Error)
d_1	-0.405 (0.11)
d_2	0.509 (0.036)
d_3	-2.11 (0.24)
d_4	4.25 (0.05)
d_5	0.667 (0.009)
d_6	-0.0947 (0.009)
d_7	-0.266 (0.023)
$\sigma_{\ln \text{CAV}2}$	0.46

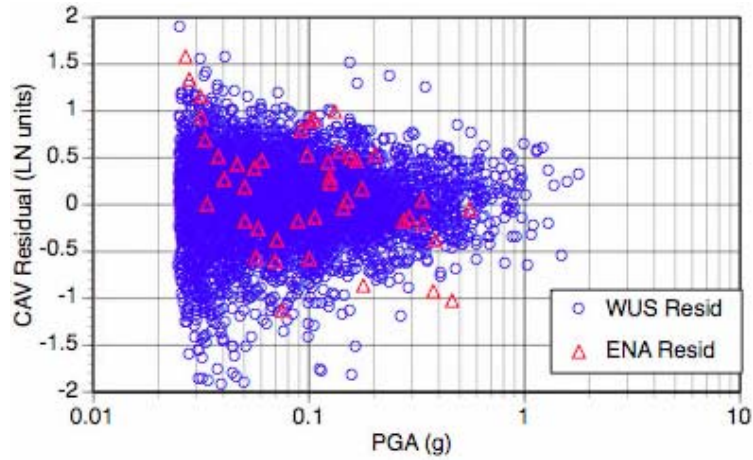


Figure 2-35
PGA Dependence of the Residuals of CAV from the Single Step Model

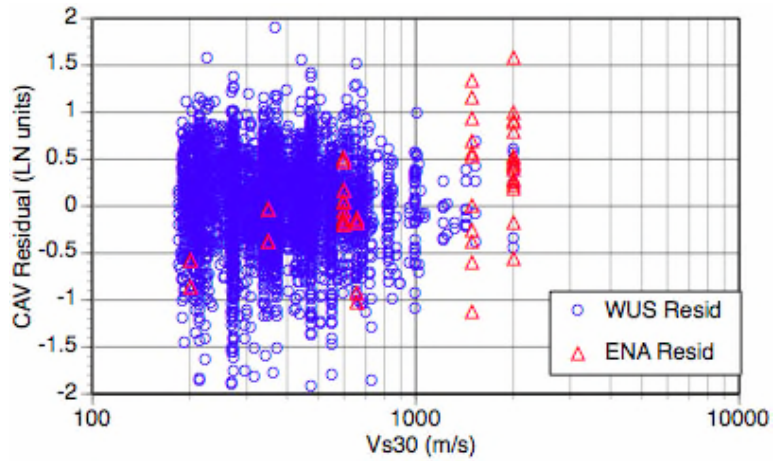


Figure 2-36
 V_{s30} Dependence of the Residuals of CAV from the Single Step Model

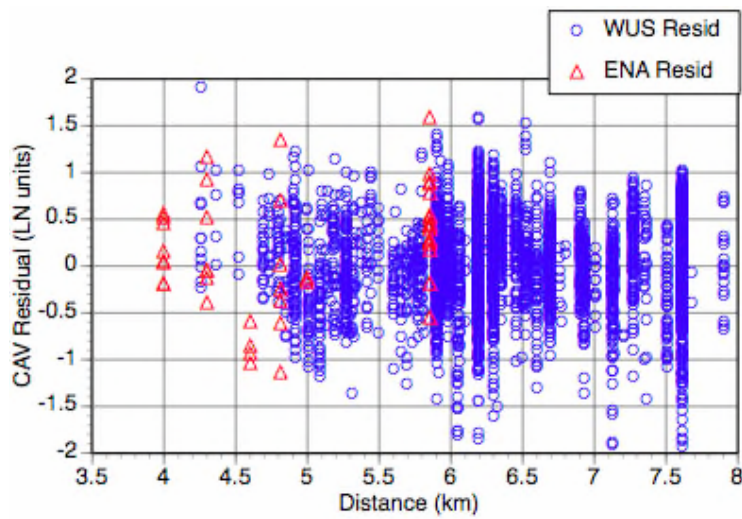


Figure 2-37
Magnitude Dependence of the Residuals of CAV from the Single Step Model

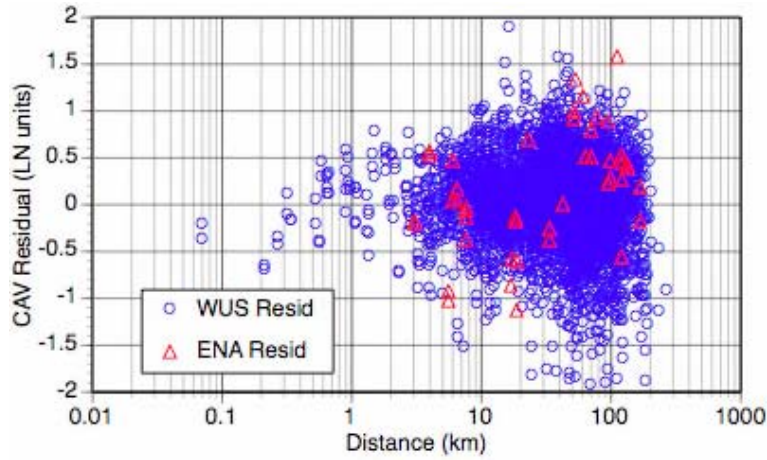


Figure 2-38
Distance Dependence of the Residuals of CAV from the Single Step Model

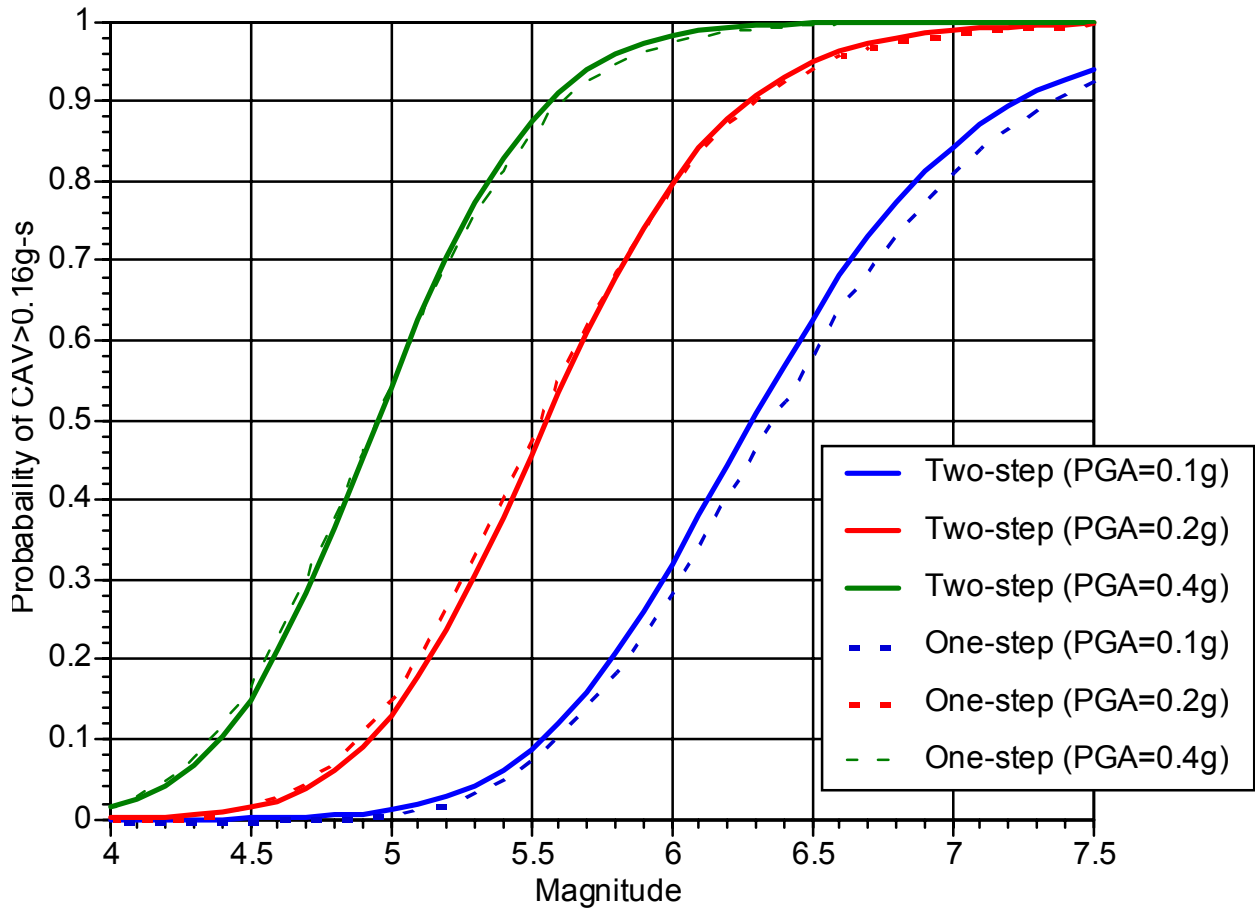


Figure 2-39
Comparison of the Probability of CAV > 0.16g-s from the Two-Step and One-Step Approaches for $V_{S30}=1000\text{m/s}$

3

APPLICATION OF THE CAV MODEL FOR RESPONSE SPECTRAL VALUES

The CAV model described above is based on the PGA. For PSHA, we need to be able to compute the CAV for response spectral values as well as for PGA.

Independent CAV Models for Spectral Acceleration

The most direct approach would be to simply derive a CAV model following the 1-Step approach used in Chapter 2, but with the spectral acceleration values in place of the PGA. This approach does not work well because the CAV as a function of the spectral acceleration will depend on the spectral shape. Since the spectral shape is very different between ENA and WUS earthquakes, the CAV predicted from WUS earthquakes will not give an estimate of the CAV for the EUS earthquakes.

In addition, the approach is to remove the events with $CAV < 0.16g\cdot s$ from the hazard, but developing separate models for the CAV for the different spectral periods leads to different earthquakes being removed from the hazard for the different spectral periods.

To avoid these two problems, an alternative approach is to use the PGA to determine the CAV and then estimate the spectral acceleration given the PGA value. This approach is described in the following section.

CAV Models for Spectral Acceleration Correlated to PGA

To estimate the effect of CAV on the response spectral values at periods other than 0 (e.g., other than PGA) requires a model of the relation between the PGA and the spectral acceleration. The spectral shape from the attenuation relation can be used to estimate the median PGA given the median spectral acceleration. In addition to the median spectral shape, we need to account for the aleatory variability of the spectral shape. Models for the correlations of the normalized residuals (epsilon values) of PGA and spectral acceleration from attenuation relations are developed.

Assuming a linear correlation, the relation between the residuals is given by:

$$\varepsilon_{SA}(f) = b_1 \varepsilon_{PGA}$$

Equation 3-1

where ε_{PGA} is the epsilon value of PGA for the time series and $\varepsilon_{SA}(f)$ is the epsilon value of spectral acceleration at frequency f . The dataset used to develop the correlation model is the

PEER NGA data set, with residuals calculated using a preliminary version of the Abrahamson and Silva (2005) model. The model coefficients were estimated using ordinary least-squares. The resulting coefficients can be found in Table 3-1. At high frequencies, the WUS b_1 values are close to unity because the WUS data does not have much high frequency content. For the EUS data with greater high frequency content, the correlation was estimated using the variability of the spectral shapes from the Saguenay earthquake data (Table 3-1).

Table 3-1
Coefficients for the Correlation of the Variability of $\ln(\text{PGA})$ and $\ln(\text{Sa})$

	WUS	EUS
Freq (Hz)	b_1	b_1
0.5	0.590	0.50
1	0.590	0.55
2.5	0.600	0.60
5	0.633	0.75
10	0.787	0.88
20	0.931	0.90
25	0.956	0.91
35	0.976	0.93

The median S_a for a given PGA value is given by:

$$\ln(S_a(f) | \text{PGA}, M, R, V_{S30}) = \ln(S_{a_{med}}(M, R, V_{S30}, f)) + b_1(f) \varepsilon_{\text{PGA}} \sigma_{\ln S_a} \quad \text{Equation 3-2}$$

The standard deviation of $\ln(\text{Sa}(f)|\text{PGA})$ is given by:

$$\sigma_{\ln S_a | \text{PGA}} = \sqrt{1 - b_1^2} \sigma_{\ln S_a} \quad \text{Equation 3-3}$$

It is important to note that the correlations listed in Table 3-1 are for the correlation of the variability of the PGA and spectral acceleration for a given magnitude and distance. While the median spectral shape can be very different for the WUS and EUS, the correlation of the variability is much more stable. This is seen by the similarity of the correlations for the WUS data and the Saguenay data.

4

METHODOLOGY FOR APPLICATION OF MINIMUM CAV IN SEISMIC HAZARD ANALYSES

The CAV models given above can be easily used to modify the results from a standard hazard analysis to remove the earthquakes that have no damage potential. The CAV filtering can be applied as part of the hazard analysis (e.g., inside the hazard integral) or it can be applied as a post process. These two approaches are discussed below.

Application of CAV Filtering During the Hazard Calculation

The most direct method for applying the minimum CAV model described above as part of the hazard calculation is to add an integral over the PGA aleatory variability. This becomes:

$$v(Sa > z) = \sum_{i=1}^{N_{source}} N_i(M > M_{min}) \int_{M=M_{min}}^{M_{maxi}} \int_{R=0}^{\infty} \int_{\epsilon_{PGA}=-5}^5 \frac{\{f_{mi}(M)f_{ri}(r, M)f_{\epsilon}(\epsilon_{PGA})\}}{P(Sa > z | M, R, PGA)} P(CAV > 0.16 | M, PGA(M, R, \epsilon_{PGA})) d\epsilon_{PGA} dr dM \quad \text{Equation 4-1}$$

where $P(CAV > 0.16 | M, PGA)$ is given by eq. 2-4,

$$P(Sa > z | M, R, PGA) = 1 - \Phi(\epsilon'_{SA}) \quad \text{Equation 4-2}$$

and

$$\epsilon'_{SA} = \frac{\ln(z) - (\ln Sa_{med}(M, R) + b_1 \epsilon_{PGA} \sigma_{SA})}{\sqrt{1 - b_1^2 \sigma_{SA}}} \quad \text{Equation 4-3}$$

For large hazard calculations, this additional integral may add significantly to the computation time. A more efficient method for applying the minimum CAV in a PSHA can be developed that avoids the need for the additional integral in the hazard.

Application of CAV Filtering in the Post Processing of the Hazard Calculation

A standard hazard analysis will yield a hazard curve, $v(Sa_{Rock}(f) > z_k)$, and the deaggregation, $Deagg(M_i < M < M_{i+1}, R_j < R < R_{j+1}, Sa(f))$. Using these two pieces of information, we can compute

the rate of occurrence of spectral acceleration over a small acceleration range from a specified magnitude and distance range:

$$\begin{aligned} & \nu(z_k < Sa_{Rock}(f) < z_{k+1}, M_i < M < M_{i+1}, R_j < R < R_{j+1}) = \\ & \nu(Sa_{Rock}(f) > z_k)Deagg(M_i < M < M_{i+1}, R_j < R < R_{j+1}, z_k) \\ & - \nu(Sa_{Rock}(f) > z_{k+1})Deagg(M_i < M < M_{i+1}, R_j < R < R_{j+1}, z_{k+1}) \end{aligned} \quad \text{Equation 4-4}$$

For more compact notation, this rate of occurrence is denoted as $\nu_{occur}(Sa_k, M_i, R_j)$.

Let ν' be the hazard curve for potentially damaging ground motions (CAV>0.16g-sec), then:

$$\nu'(Sa_{Rock}(f) > z_n) = \sum_{i=1}^{N_m} \sum_{j=1}^{N_r} \sum_{k=n}^{N_a} \nu_{occur}(z_k, M_i, R_j) P(CAV > 0.16g - s | z_k, M_i, R_j) \quad \text{Equation 4-5}$$

In words, the CAV filtering of the hazard is implemented by first breaking the hazard curve back down into rates of occurrence of scenario earthquakes (M,R,Sa). From these scenario earthquakes, we can compute the epsilon for the given Sa. Then using this information, we can then compute the probability that this scenario will lead to a CAV value greater than 0.16g-sec. This probability is then multiplied by the rate of the scenario. We then sum up the rates of all the scenarios with spectral accelerations greater than our test value, resulting in the CAV filtered hazard.

The hazard curves described above are for “outcropping rock”; however, the CAV model was developed using surface (“soil” or “rock”) values of spectral acceleration. When calculating the probability of CAV>0.16g-sec, it is necessary to first scale the SaRock to SaSoil using the site amplification factors, and then use the SaSoil values as input to the CAV model since the CAV model was developed for surface ground motions.

$$\begin{aligned} \nu'(Sa_{Soil}(f) > z_n) = & \sum_{i=1}^{N_m} \sum_{j=1}^{N_r} \sum_{k=1}^{N_a} \nu_{occur}(z_k, M_i, R_j) \\ & P(CAV > 0.16g - s | Sasoil_k(z_k), M_i, R_j) \end{aligned} \quad \text{Equation 4-6}$$

5

EXAMPLE APPLICATION

As an example, the CAV filtered hazard is computed for a CEUS rock site using the USGS (Frankel et al. 2002) smoothed seismicity and the Toro et al (1997) attenuation relation. No fault sources were included. In this example, the CAV filtering is applied inside the hazard integral using eqs. 4-1, 4-2, and 4-3. The CAV is modeled using the two-step approach from Chapter 2.

The hazard curves for 20 Hz spectral acceleration are shown in Figure 5-1 with and without the CAV filtering. The effect of removing the events with CAV less than 0.16g-sec is to flatten the hazard curve at small ground motion levels. There is little effect on the hazard curve for high ground motion levels since these levels will be associated with CAV values greater than 0.16g-sec. The uniform hazard spectrum for a probability level of 1E-4 is shown in Figure 5-2 with and without the CAV filtering. At a hazard level of 1E-4, the UHS is reduced by about 10-25% due to CAV filtering. This example is for a site that is not close to either the Charleston or New Madrid sources. For sites close to these sources, the effect of the CAV filtering on the low frequency part of the UHS will be smaller since the ground motions that form these larger magnitude earthquakes will have large CAV values.

The example deaggregation for 20 Hz spectral acceleration for a hazard level of 1E-4 is shown in Figure 5-3 with and without the CAV filtering. The effect of the CAV filtering is to remove the contribution from smaller magnitudes, shifting the peak in the deaggregation to larger magnitudes and larger distances. For the PSHA using a fixed lower bound moment magnitude of 4.6, there is a significant contribution from M4.6-5.0, but these are removed in the CAV filtered hazard.

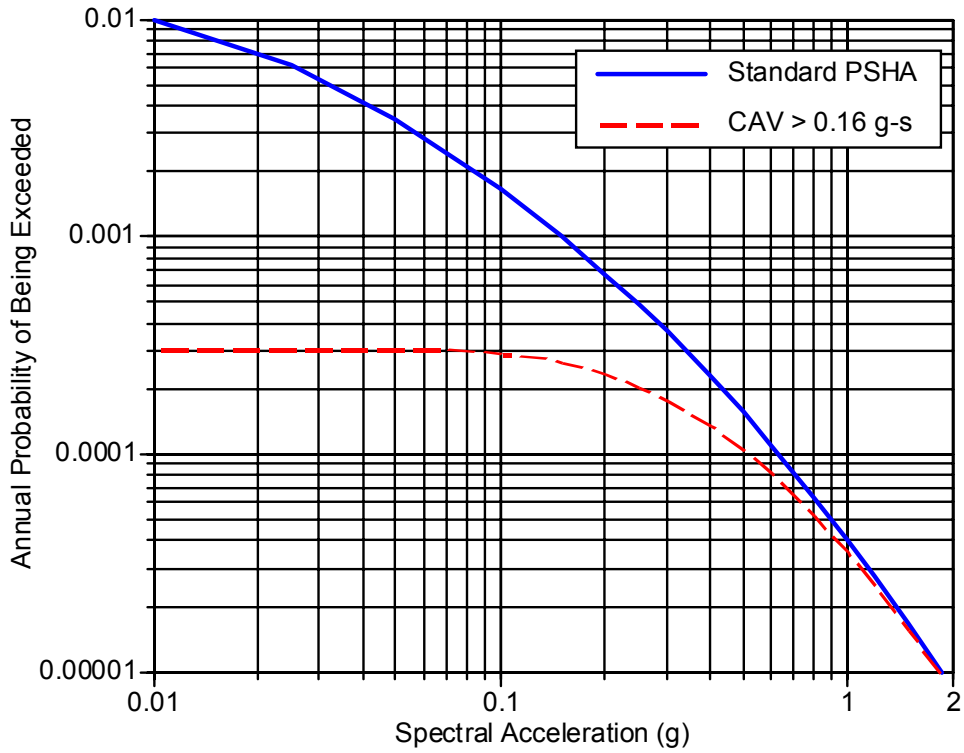


Figure 5-1
20 Hz Hazard Computed With and Without CAV Filtering

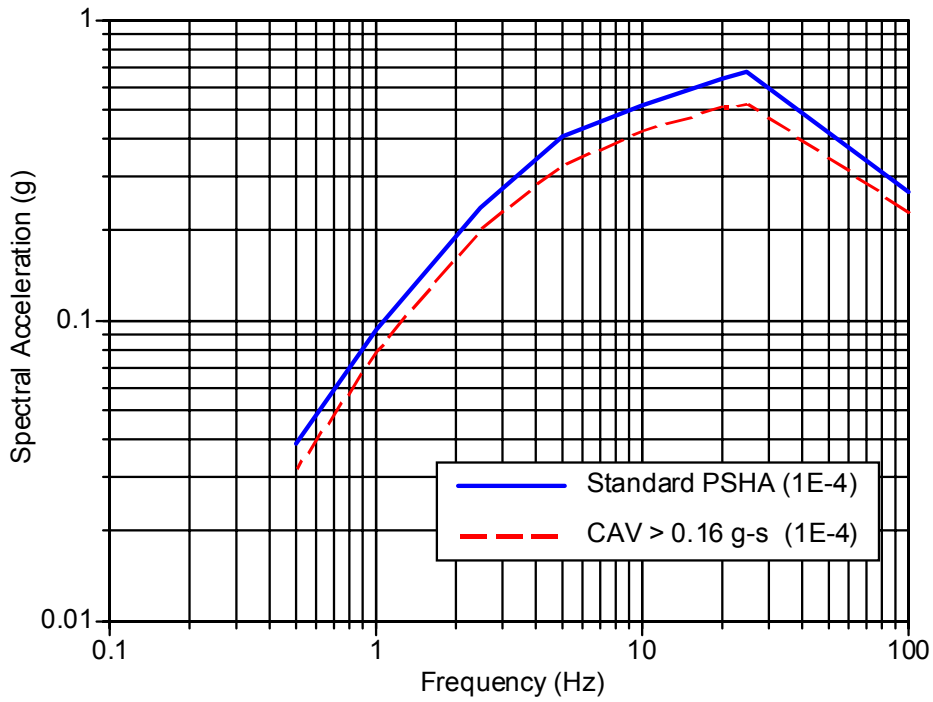


Figure 5-2
UHS for 1E-4 With and Without CAV Filtering

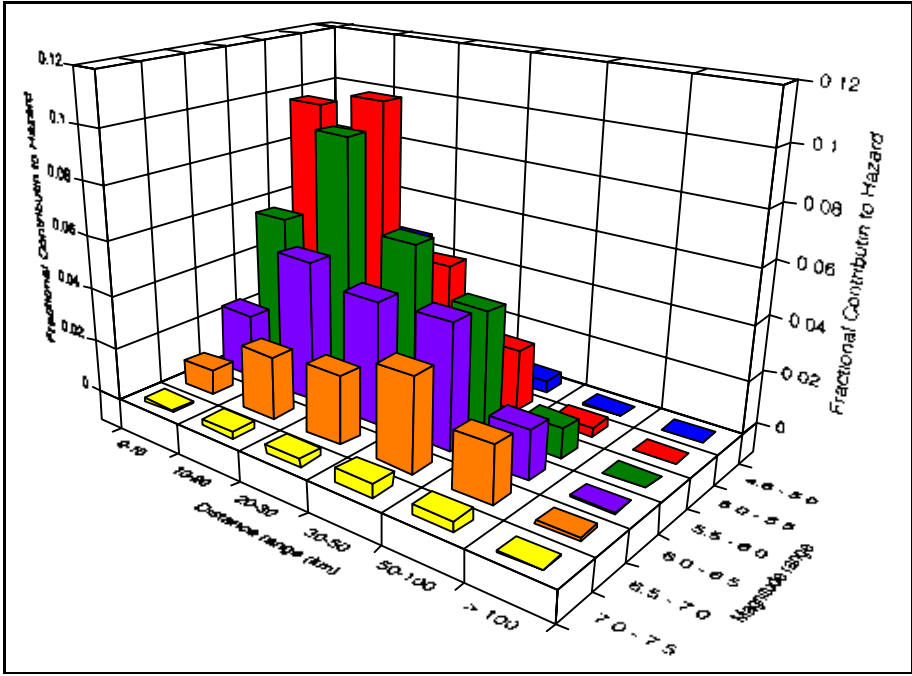
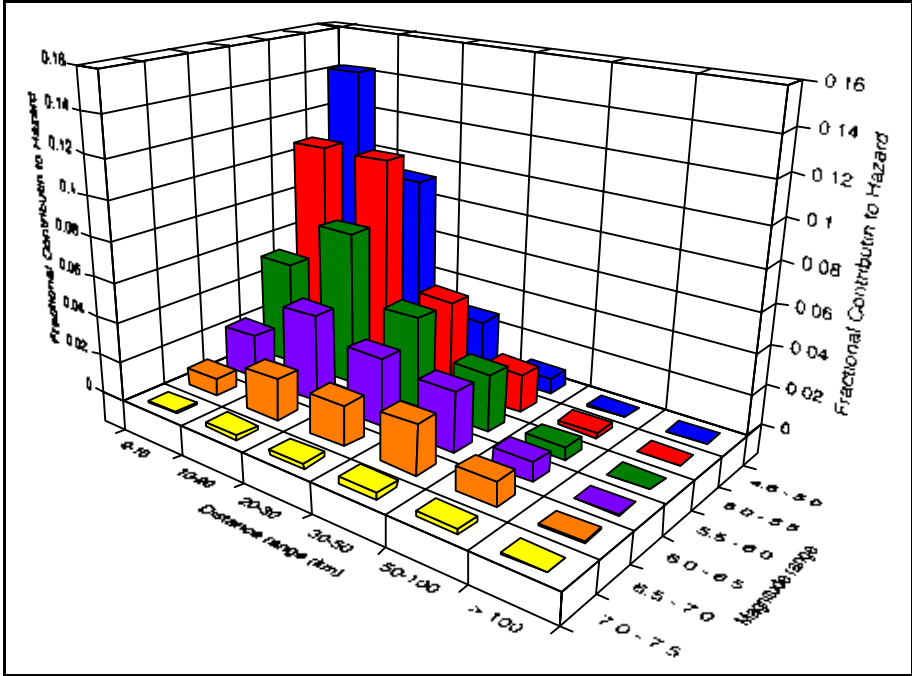


Figure 5-3
Deaggregation of 20 Hz Spectral Acceleration Hazard for 1E-4.
The upper plot is the standard PSHA. The lower plot is the CAV filtered deaggregation.

6

CONCLUSIONS

This study provides the technical basis for establishing the appropriate distribution of low magnitude earthquakes for use in probabilistic seismic hazard computations for nuclear power plant applications. Current seismic hazard methods generally utilize a lower bound body wave magnitude cut-off value of 5.0 (approximate moment magnitude of 4.6) to integrate the probabilistic seismic hazard. This lower bound magnitude cut-off level was a conservatively defined value based on several past research studies whose objective was to estimate the damage potential of small earthquakes. A much more complete and technically defensible characterization of the damage potential for small earthquakes was determined to be the cumulative absolute velocity (CAV). A CAV value of 0.16 g-sec was defined in past studies to characterize a conservative estimate of the threshold between damaging earthquake motions and non-damaging earthquake motions for well-engineered structures. Based on the review of available CEUS and WUS data, CAV is modeled as a function of the uniform duration, magnitude, peak ground acceleration, and site shear wave velocity. The application of a minimum CAV value significantly reduces the contribution of small magnitude earthquakes to the total hazard leads to a controlling earthquake that more correctly represents the contributions of potentially damaging earthquakes to the hazard at a site. At high frequencies, the magnitude of the controlling earthquake increases from near magnitude 5.25 for the fixed lower bound moment magnitude 4.6 to magnitude 5.8 by applying the CAV model.

7

REFERENCES

Abrahamson, N. A. and W. J. Silva (2005). *Preliminary Results of the A&S 2005 Attenuation Relation*, presented at the USGS workshop on Attenuation Relations to be used in the USGS National Seismic Hazard Maps, Menlo Park, CA, October 24, 2005,

Bolt, B.A. (1973). *Duration of Strong Ground Motion*, Proc. Fifth World Conf. Earth. Eng., Rome, 1304-1307.

EPRI (1993). *Guidelines for Determining Design Basis Ground Motions*, EPRI Report TR-102293, November 1993.

Frankel, A.D., Petersen, M.D., Muller, C.S., Haller, K.M., Wheeler, R.L., Leyendecker, E.V., Wesson, R.L., Harmsen, S.C., Cramer, C.H., Perkins, D.M., and Rukstales, K.S., (2002), *Documentation for the 2002 Update of the National Seismic Hazard Maps*: U.S. Geological Survey, Open-File Report 02-420.

McCann, M.W. and J.W. Reed (1989). *Proceedings: Engineering Characterization of Small-Magnitude Earthquakes*, EPRI Report NP-6389, June 1989.

National Earthquake Information Center. <http://neic.usgs.gov>, 2005.

O'Hara, T.F. and J.P. Jacobson (1991). *Standardization of the Cumulative Absolute Velocity*, EPRI Report TR-100082, Tier 2, December 1991.

PEER NGA Strong Motion Database. <http://peer.Berkeley.edu/NGA>, 2005.

Reed, J.W. and R.P. Kennedy (1988). *A Criterion for Determining Exceedance of the Operating Basis Earthquake*, EPRI Report NP-5939, July 1988.

Toro, G.R., N.A. Abrahamson, and J.F. Schneider (1997). *Model of Strong Ground Motions from Earthquakes in Central and Eastern North America: Best Estimates and Uncertainties*, Seism. Res. Let., 68, 58-73.

A

COMMENTS AND RESPONSES TO NRC REQUESTS FOR ADDITIONAL INFORMATION (RAIs)

The NRC submitted 15 RAIs related to the G1.2 Task on June 1, 2006. These RAIs were titled “Section 2.0 – Combined NRC RAI Comments on EPRI Report 1012965 *Use of CAV in Determining Effects of Small Magnitude Earthquakes on Seismic Hazard Analyses (G1.2)*”. The industry responses and resolutions for these 15 RAIs are documented below.

NRC Comment/Question:

- 2.1 Provide CAV-filtered hazard curves for the twenty-eight CEUS reactor sites so that NRC staff can assess the impact of using CAV for determining the effects of small earthquakes on seismic hazard analysis. (Have the hazard curves labeled consistently so they can be compared with the curves provided in response to RAIs G1.1 and G1.2?)

Industry Response/Resolution:

- 2.1 These CAV filtered hazard curves for the 28 sites will be provided by July 15, 2006 in a separate report under the G1.1 Task.
-

NRC Comment/Question:

- 2.2 Cumulative Absolute Velocity (CAV) methodology and CAV threshold of damage (0.16g-sec) were standardized in the EPRI Technical Report (TR 100082) published in 1991. The author stated that “this value was determined by the Whittier earthquake (record no 281) which has the lowest CAV value associated with an earthquake of Intensity VII.” The CAV associated with the record no. 281 is 0.28 g-sec, corresponding to a MMI VII site intensity, which is conservatively assumed to have damage potential to buildings of good design or construction. To demonstrate the conservativeness of the threshold, the report also compared industry buildings with different design standards and concluded that the threshold is “a factor of five lower than the lowest CAV value associated with documented damage to an industrial/power facility and it is about a factor of three lower than the lowest CAV value associated with documented damage to buildings of good design and construction.”

Although the report did not clearly address why the CAV threshold was adjusted from 0.28 to 0.16 g-sec, a CAV of 0.177 g-sec (record no. 56) from the Hollister earthquake (3/9/1949, ML=5.3, site MMI=VII) was referenced in the report, implying that the 0.16 g-sec was proposed by referring 0.177 g-sec, which also corresponds to an site MMI of VII.

Following questions are related to the threshold of 0.16 g-sec.

- 2.2a. Modified Mercalli Intensity Scale (MMI) is descriptive in nature. An MMI category assigned to a site varies based on different observers, and sometimes it was difficult to assign an MMI to a site because different structures behaved differently, such as high rise and lower rise buildings in Mexico City following the 1985 Michoacan earthquake. However, CAV threshold is a quantitative measure of the damage threshold. Please provide the basis for selecting the 0.16 g-sec threshold as a quantitative measure of no damage to structures, in view of the qualitative nature of assigning an MMI to a site; also, please justify the limitation imposed by simplifying the complexity of ground motions into a single parameter of CAV.
- 2.2b. In view of significant increase of strong motion earthquake recordings near industrial sites since 1980, please justify the usage of 0.16 g-sec as a conservative threshold for damage, by providing examples from recent strong motion recordings (from recordings near damaged and undamaged facilities) to show that 0.16 g-sec is still applicable as a conservative threshold for damage.

Industry Response/Resolution:

2.2a and b.

As discussed at the May NRC meetings, the CAV level of 0.16 g-sec was set on a conservative basis for the OBE Exceedance program and accepted by the NRC within Reg Guide 1.166. There is no reason to believe that any new data from recent earthquakes would change that CAV value. At the May 11-12 meetings at the NRC, we agreed to draft a white paper documenting our thoughts on this subject. That white paper was sent directly to the NRC and is provided below as the response to this two part RAI question.

White Paper:
NRC Request on CAV Damage Threshold

This document provides a response to an NRC information request on the acceptability of the CAV value of 0.16 g-sec as a conservative exceedance threshold for developing a conditional probability function that allows non-damaging earthquakes to be filtered from a seismic hazard analysis using a smooth transition function.

Introduction

The NRC issued 14 RAIs to NEI on April 27, 2006 related to the G1.2 project report “Use of Minimum CAV in Determining Effects of Small Magnitude Earthquakes on Seismic Hazard Analysis”. The first RAI within this NRC letter addressed the use of the CAV threshold as a damage parameter (the CAV threshold level is 0.16 g-sec) in the G1.2 project to filter non-damaging earthquakes from a seismic hazard analysis. The RAIs were reissued, with some clarifications, on June 1, 2006. The full request from the NRC is contained in the NRC correspondence, but the partial text of the two-part CAV threshold request is as follows:

- a) ...”Please provide the basis for selecting the 0.16 g-sec threshold as a quantitative measure of no damage to structures, in view of the qualitative nature of assigning an MMI to a site”...“also please justify the limitation imposed by simplifying the complexity of ground motions into a single parameter of CAV.”
- b) “In view of the significant increase of strong motion earthquake recordings near industrial sites since 1980, please justify the continued usage of 0.16 g-sec as a conservative threshold for damage by providing examples from recent strong motion recordings...”.

These two requests were discussed at the May 11-12, 2006 new plant seismic issues meeting at the NRC. The industry (NEI, EPRI and EPRI consultants) presented the position that the use of the CAV parameter and the selection of the 0.16 g-sec CAV threshold level were chosen in the G1.2 project specifically to eliminate any debate on (1) what parameter should be used to best characterize the threshold of damage for NPP equipment/structures, and (2) what level of that parameter conservatively defines the value of that threshold.

An EPRI research project (Reference 1 and 2) conducted in the late 1980’s and early 1990’s provides the necessary information for the response to part a) of the request above. Reference 1 describes a variety of damage parameters considered in the study, and the basis for selecting the CAV as the parameter with the best correlation to potential damage. Reference 2 describes the process for computing the CAV and the basis for the 0.16 g-sec threshold. The NRC participated in the review of this project and endorsed its results in RG 1.166 as part of the OBE exceedance criteria.

Regarding part b) of the RAI, the industry presented its position in the May meeting that there is no known earthquake occurrence/data that contradicts the basis for the CAV threshold criterion of RG 1.166 and that use of the CAV parameter along with the 0.16 g-sec threshold remain valid. The requested additional research to study the implications of strong motion recordings near industrial sites since 1980 is considered by the industry to be unwarranted from a technical standpoint (the CAV threshold was set at a very conservative level) and would also be a burden from the resource and schedule perspective for the new plant seismic program. At the conclusion of the NRC meetings, the NRC requested that the industry document and submit their position presented at the meeting together with a brief summary to address request a) on the basis for selecting the 0.16 g-sec CAV. In addition, the NRC commented that they would independently research the question relating to the new earthquake effects on the CAV value to determine if there was a more specific basis for requesting a detailed assessment of this issue from the industry. The following information represents the response to request a) above.

Selection of the CAV Threshold Damage Value

The CAV concept was developed in Reference 1, which concluded that the CAV was the best single parameter for determining the damage threshold of earthquake ground motion. The procedure for determining the CAV was further refined in Reference 2 which standardized the computational algorithm to be used to determine the CAV value associated with a given free-field acceleration time-history record. The CAV is the integration of the absolute value of ground acceleration over successive one-second intervals of a free-field acceleration time-history for which the absolute value of the recorded acceleration exceeds 0.025 g. Over 177 seismic records were used in the study

(Reference 2) along with a Modified Mercalli Intensity (MMI) value assigned to each record site. In general, the assignment of the MMI intensity associated with each record site was based on published isoseismic maps for a given earthquake event. In some cases, the MMI intensity associated with a given record site was based on actual damage noted in the vicinity of the site. Reference 1 provides full documentation of the sources used for determination of MMI intensity for the record sites. The CAV value was computed for each site record and then correlated with the assigned site intensity value. The threshold of damage potential was chosen conservatively as MMI intensity VII for which there is “negligible damage to buildings of good design and construction” (see Reference 1 for definition). Reference 2 determined that the threshold CAV value associated with MMI VII was 0.16 g-sec. This value was chosen as the lowest CAV value associated with site MMI intensity VII, which is the record associated with (i.e., closest to) the Pasadena Power Plant in the 1987 Whittier earthquake. The plant had no damage due to the earthquake.

Figure 1 shows the entire set of 177 CAV values from Reference 2 plotted against the assigned site MMI intensity. Note that CAV values as high as 3 occur for sites with MMI site intensity VII. The goal of the studies documented in References 1 and 2 was to establish a screening value which could be used as justification for continued nuclear plant operation following an earthquake, given that the threshold CAV determined from site (free-field) records was not exceeded.

Reference 2 identifies the records associated with the El Centro Steam Plant during the 1979 Imperial Valley earthquake as having the lowest CAV values (0.77 - 0.94) associated with minor damage to a power plant facility. The site intensity was identified as MMI VIII. There were four horizontal strong motion records associated with the plant site 1) two records from the USGS Differential Array (2400 ft. from Unit 4 of the plant) and 2) two records from the USGS El Centro Array No. 8 (4000 ft. from Unit 4 of the plant). The noted plant damage was structural only, being minor concrete cracks and buckling of the boiler frame braces. The plant operating units were fully functional following the earthquake. The El Centro Steam Plant is one the reference data sites used by the Seismic Qualification Utility Group (SQUG) to establish the Unresolved Safety Issue (USI) A-46 resolution. The minimum CAV value for this plant is identified in Figure 1 as the lowest value for power plant structural damage (EC Array No. 8, CAV = 0.77 & 0.82; Diff. Array, CAV = 0.91 & 0.94). The other lower CAV values indicated in Figure 1 for MMI VIII are for commercial building structures with minor structural damage (CAV > 0.54).

Reference 1 concluded that power plants and other heavy industrial facilities can sustain ground motion levels associated with MMI VIII site intensities and remain functional. The threshold CAV value determined in Reference 2 was purposely chosen to be a conservatively low value associated with MMI VII records representing a non-damaging level to be used as a screening value for continued operation of a nuclear plant following an earthquake.

In general, the CAV is a function of the duration of the strong motion portion of the time-history record. If the cumulative value of the CAV is plotted as a function of time using the equation,

$$CAV(t) = \sum_i \int_{t_i}^{t_{i+1}} W_i |a| dt$$

where $S_i = 0$ for $|a| < 0.025g$ and $W_i = 1$ for $|a| \geq 0.025g$ and zero otherwise, the generation of the total CAV value may be compared to the acceleration time-history. For this calculation, the integration limits, t_i , are taken as integer values of time in seconds. Figure 2 shows a cumulative CAV function plot corresponding to the closest free-field acceleration records associated with the El Centro Steam Plant. This type of presentation indicates that the strong motion portion of each time-history record yields a region where the CAV value accumulates at an approximate constant rate.

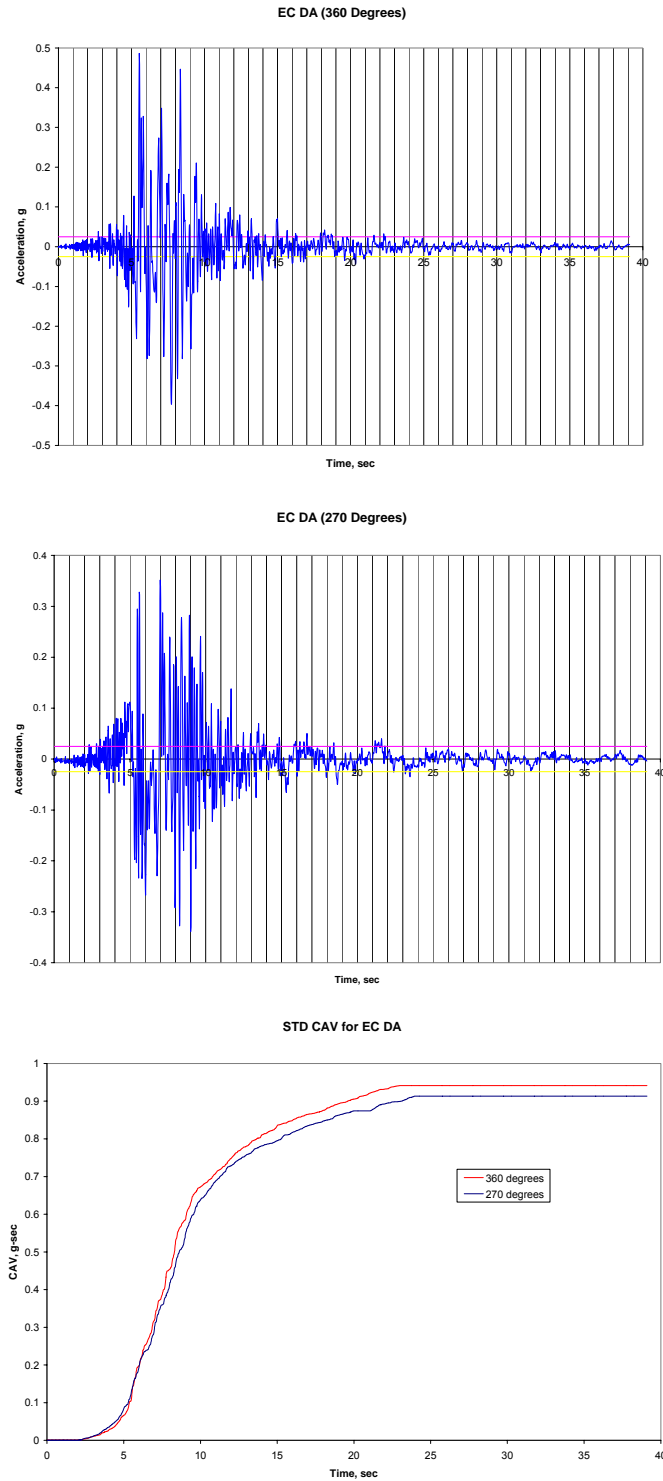


Figure 2. Time-History Records and Computed CAV Values Associated with the El Centro Steam Plant (Differential Array, 1979 Imperial Valley, CA Earthquake; closest record to plant)

As can be noted in Figure 2, the CAV for the El Centro Steam Plant includes the strong motion portion (5-10 sec) that contributes approximately 60% of the total CAV value. The remaining portion of the CAV value is due to the initial 2-5 sec rise time and the 10-23 sec decay time of the records. Thus, the computed CAV value is always larger than the strong motion contribution resulting in a conservative damage measure when used as a low bound exclusion criterion.

The damage threshold CAV value of 0.16 g-sec, selected in Reference 2, was based on the observed negligible structural damage associated with MMI VII for buildings of good design and construction. Since power plants have been subjected to earthquake motions with observed MMI VIII levels and have remained functional, the selected threshold CAV value of 0.16 g-sec which is associated with MMI VII can also be interpreted as a conservative measure of threshold functional damage. If a motion, either a design time-history or an actual acceleration record, is associated with a given power plant site, then we can state, with high confidence, that no functional damage should occur to components within that plant (given the primary caveats are satisfied, i.e. adequate anchorage, sufficient restraint, lack of spatial interaction, etc.). This is the underlying basis for the CAV threshold criteria included in Regulatory Guide 1.166 as an optional method for determining Operating Basis Earthquake exceedance in the case of a seismic event occurring in the vicinity of an operating nuclear power plant.

Conclusion

The CAV threshold value of 0.16 g-sec, included in RG 1.166 and based on the documented EPRI studies, represents a very conservative value for use as a threshold in developing a conditional probability function that filters non-damaging earthquakes (i.e., low Magnitude events) from the seismic hazard analysis.

References:

1. "A Criterion for Determining Exceedance of the Operating Basis Earthquake", EPRI NP-5930, July 1988.
 2. "Standardization of the Cumulative Absolute Velocity", EPRI TR-100082, December 1991.
-

NRC Comment/Question:

- 2.3 Ground motion recordings included in the WUS data are mostly recorded in the lower shear wave velocity soils (the largest cluster is corresponding to 200-300 m/s) and higher attenuation crust. How can this WUS CAV model be applied to the eastern US, which is different in term of surface soil shear wave velocities and attenuation characteristics?

Industry Response/Resolution:

- 2.3 The CAV model depends on the ground motion level. The ground motion is strongly dependent on the surface Vs and attenuation characteristics, so the CAV dependence on these variables is accommodated through the PGA correlation. A detailed explanation of this is given on pages 1-3 to 1-6.

NRC Comment/Question:

- 2.4 Since previous earthquakes have demonstrated that structural damage is closely correlated to surface soil type, if CAV is not sensitive to a soil type please explain how can it be used to as a single parameter for structural damage?

Industry Response/Resolution:

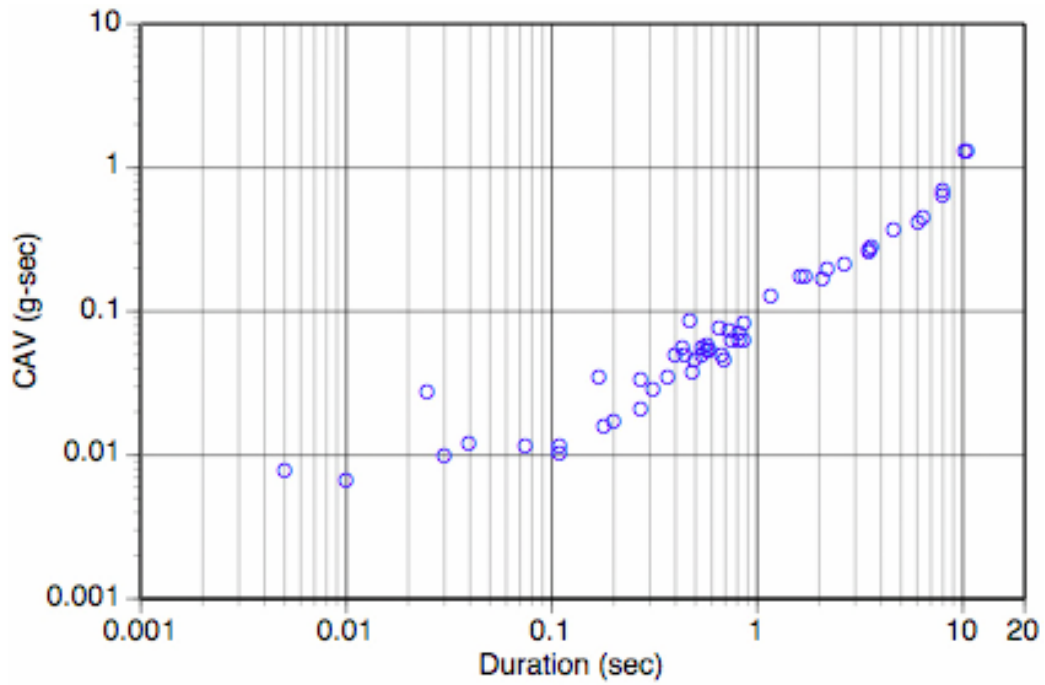
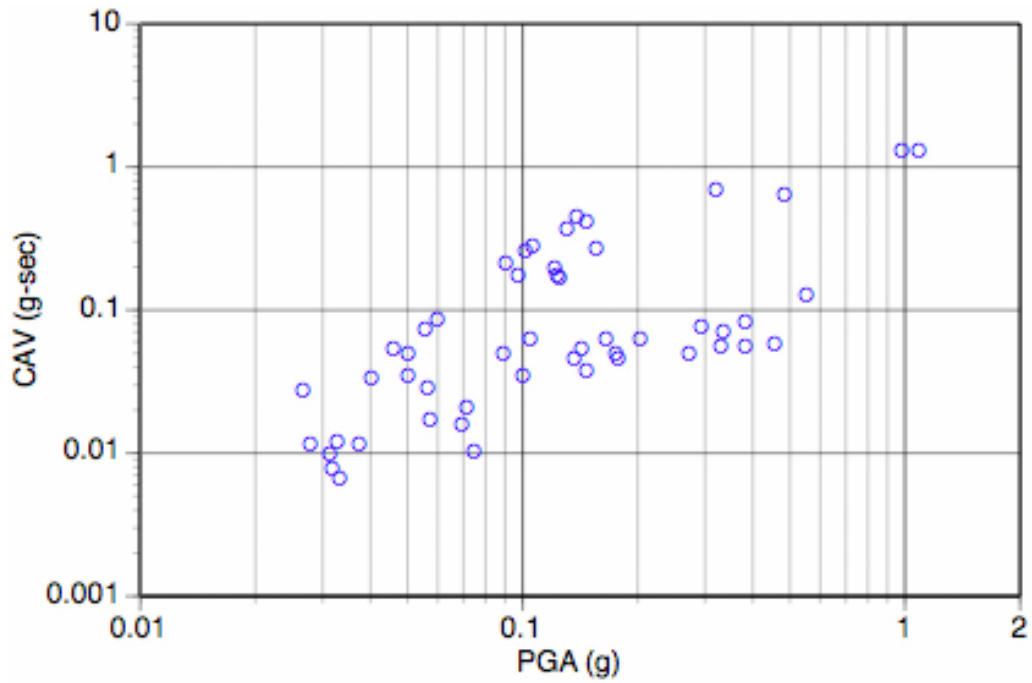
- 2.4 CAV is sensitive to soil type, but this is accommodated through the PGA dependence.

NRC Comment/Question:

- 2.5 The report indicates that the CAV model based on WUS data strong motion data set is applicable to the EUS because no significant bias in terms of CAV residuals distribution for the CEUS (figure 2-11 in the report). The residuals are the estimates of experimental error obtained by subtracting the observed responses from the predicted response. How are the CAV distributions with respect to uniform durations and PGAs for the CEUS?

Industry Response/Resolution:

- 2.5 This Question was not clear and was clarified at the May 12 meeting. Plots of the CAV data from the EUS are plotted as functions of PGA and uniform duration. The plots of the EUS CAV data vs PGA and duration are shown below:



NRC Comment/Question:

- 2.6 Author states that “CAV is highly variable for recordings with PGA > 0.025 g threshold” for the CEUS data set. If so, why it is appropriate to apply the WUS CAV model to the CEUS? The CEUS data set has a total of 54 components from 9 events. CEUS data set was used with different PGA cutoff values, 0.03g for comparison with WUS CAV model, 0.04g when compared WUS CAV residuals, and 0.05g when compared duration residuals with WUS. What is the justification to compare CAV related model parameters with different cutoff PGA values? How many of those 54 components are still left after each change of the cutoff values?

Industry Response/Resolution:

- 2.6 The goal of the study is to develop a CAV model that is accurate for predicting the $P(\text{CAV} > 0.16\text{g-s})$. Since CAV is only defined for $\text{PGA} > 0.025\text{g}$, it varies greatly in terms of the log (CAV) as the PGA just crosses the 0.025g level. This large variability is not relevant for the problem here, so we don't want to focus on residuals for parts of the model that are not relevant.

To avoid this, we used only EUS PGA values greater than 0.03g.

The report will be revised to show all of the residuals (for all PGA values). See Figures 2-30, 2-31, 2-32, and 2-33.

NRC Comment/Question:

- 2.7 Please explain why the numbers of strong motion components used are different, the attached table has 4252 components, but the report indicates a total number of 4422.

Industry Response/Resolution:

- 2.7 The data file was updated and the new total number is 4422. A new data file is enclosed. It is now consistent with the text.
-

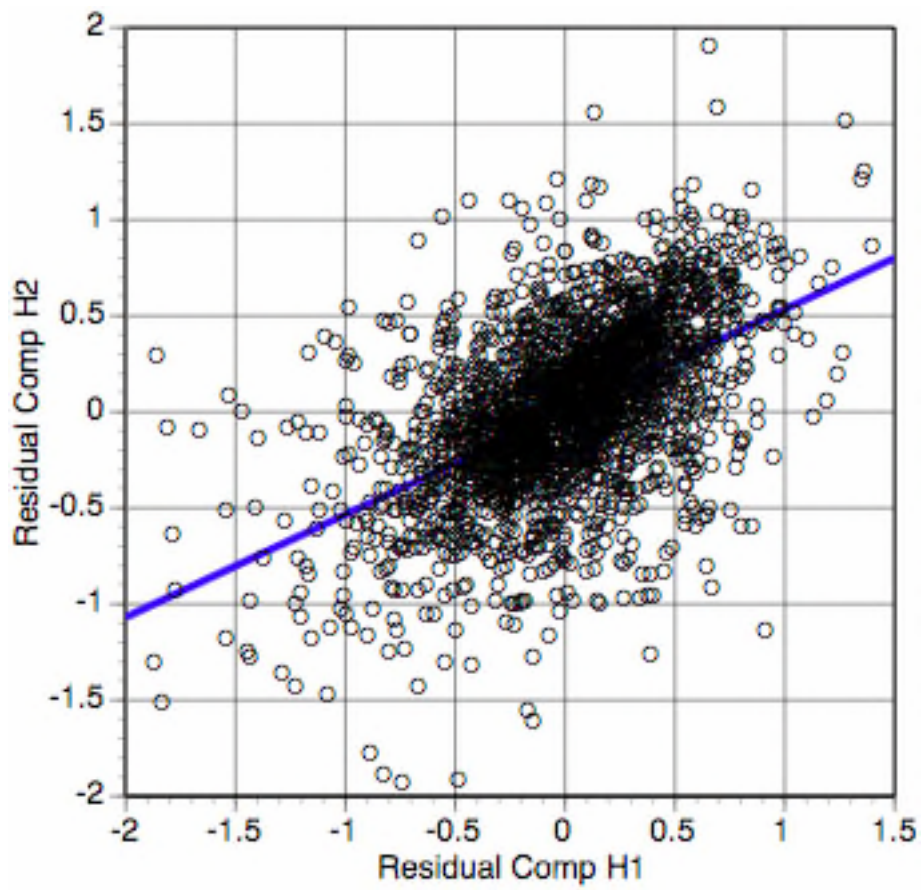
NRC Comment/Question:

- 2.8 Please clarify which component of ground motion recordings is used during the CAV modeling. If both components are used, are their correlations being considered in the modeling?

Industry Response/Resolution:

- 2.8 The two horizontal components are used. The correlation of components was not considered. The effect of the correlation will have no impact on the median, but will have a small effect on the standard deviation.

The correlation of the residuals from the two horizontal components for the combined WUS and ENA data sets is shown below. The correlation coefficient is 0.27.



NRC Comment/Question:

- 2.9 Taiwan, Turkey and Japan are quite different in tectonic settings from the west US. Please justify why the data from those regions can be used in combination with west US data to model the CAV.

Industry Response/Resolution:

- 2.9 The tectonic differences are accommodated in the ground motion level (here PGA).

NRC Comment/Question:

- 2.10 In Figures 2-8, 2-9 and 2-20, median CAV model for $V_s=600$ m/s for different magnitudes and PGAs, and uniform duration for PGAs were shown. How many strong motion components are available for $V_s = 600$ m/s? Why use only $V_s=600$ m/s subdata set?

Industry Response/Resolution:

- 2.10 $V_s=600$ m/s is used as an example just to keep the plots simple. This does not imply that only $V_s=600$ m/s data was used. All of the data was used and the dependence on V_s was estimated

NRC Comment/Question:

- 2.11 In Table 2-2, an earthquake with magnitude of 4.3 was recorded both at the station 2627A and 2627B. Are these two stations at the same site? If they are, why the V_s30 s are different?

Industry Response/Resolution:

- 2.11 These stations are both at the Franklin Falls dam. Station 2627A is located downstream and station 2627B is located on the abutment. The differences in the V_s30 values occur because of the different locations of the stations.

Additional station information was added to table 2-2 to make this clear. .

NRC Comment/Question:

- 2.12 Please explain the rationale for the functional forms of Equation 2-1 used to predict CAV based on duration, magnitude, and shear wave velocity, and of Equation 2-2 used to predict uniform duration using PGA, Vs30 and magnitude?

Industry Response/Resolution:

- 2.12 By its definition, CAV is the average acceleration times the duration. Since we are using the PGA as a predictive parameter (we have to consider the correlation of CAV and ground motion level), we expect CAV to depend strongly on duration.

By making a model that is based on duration, allows for the possibility of modifying the CAV model for regional differences in the duration models.

The text has been modified to show the rationale for the selection of the functional form. See Pages 2-8 and 2-9 and pages 2-14 to 2-17.

NRC Comment/Question:

- 2.13 Please explain the relative significance of different variables in the prediction equations for both CAV and uniform duration (Equations 2-1 and 2-2) and provide the statistics for each of the coefficients (variables).

Industry Response/Resolution:

- 2.13 The asymptotic standard errors of the parameters will be added to the report. See Tables 2-3, 2-4, and 2-5.

NRC Comment/Question:

- 2.14 Please explain why the distance factor is not explicitly expressed in the Equation 4-1.

Industry Response/Resolution:

- 2.14 This question was not clear since eq 4-1 does have distance. At the May 12 meeting, this was clarified. The intent was to ask why the CAV model not depend on distance. While CAV would depend on distance, the distance dependence is accommodated through the PGA dependence.

NRC Comment/Question:

- 2.15 Is CAV also dependent on the site location relative to the fault and fault types, like other ground motion parameters, e.g., PGA? If yes, what are the contributions from those factors?

Industry Response/Resolution:

- 2.15 Again, CAV may depend on these parameters, but the effects of these parameters are captured by the PGA. Since CAV must be dependent on the ground motion, we don't need to put these factors into the CAV model.
-

B

EMPIRICAL EARTHQUAKE DATA SETS USED FOR CAV MODELS

WUS and CEUS ground motion data sets used within this study are contained as files CAV_WUS_DATA_V2.xls and CAV_EUS_DATA_V2.xls. on the enclosed CD.